F-AM-A1 DOES SARCOMERE SHORTENING OCCUR IN STEPWISE FASHION? G.H. Pollack, T. Iwazumi, H.E.D.J. ter Keurs, and E. Shibata,* Departments of Anesthesiology and Bioengineering, RN-10, University of Washington, Seattle, Wa. 98195

Sarcomere shortening was measured in isometric contractions in both single fibers of frog semitendinosus muscle, and in trabeculae and papillary muscles isolated from rat hearts. Sarcomere length was computed on-line from the diffraction pattern with a resolution of 5 nm. The computation was performed 5 times per msec. In some experiments, a kymographic technique was used to obtain simultaneous and independent evaluation of the time course of shortening; the two techniques gave similar results.

Sarcomere shortening measured in any sampled area (diameter 180 μm) rarely occurred smoothly; shortening was generally punctuated by brief periods during which no change of sarcomere length occurred. Such "plateaus" in the shortening pattern occurred at sarcomere lengths which did not vary appreciably from contraction to contraction in any one region along the muscle; however, there was variation from region to region. The spacing between plateaus was frequently between 40 and 50 nm. Plateau duration was generally several milliseconds, although some plateaus persisted as long as 20 msec. The transitions between periods of steady shortening and no shortening usually occurred within 1 msec, and frequently within several hundred microseconds.

A basic feature of the cross-bridge theory is that the action of one cross-bridge is not directly coordinated with the action of any other. We find that regions of muscle encompassing 10^{11} bridges can start or stop shortening virtually simultaneously. To reconcile the theory with our observations it appears necessary to invoke a mechanism by which the action of all bridges is turned on or turned off synchronously; alternatively, the theory may be incorrect.

F-AM-A2 DO SARCOMERES ASSUME DISCRETE LENGTHS? T. Iwazumi, H.E.D.J. ter Keurs, and G.H. Pollack, Departments of Anesthesiology and Bioengineering, University of Washington, RN-10, Seattle, Wa. 98195

Optical diffraction patterns obtained from single fibers of striated muscle consist of a central band straddled by a series of parallel, higher order bands. The spacing between the central band and the nearest (first order) band is inversely proportional to striation spacing. On close inspection, however, it appears that each order is not simply a diffuse band but consists of a series of closely spaced but clearly separate lines contained within the band. Since the spacing between the central order and each of the lines is slightly different, the most direct interpretation of such a diffraction pattern is that muscle contains a series of several slightly different sarcomere lengths; i.e., that sarcomere lengths take on certain discrete values, but none in between these.

We have recorded diffraction patterns from single fibers of frog semitendinosus muscle in two ways. The time course of a "slice" of the pattern normal to the bands was obtained as Cleworth and Edman (J. Physiol., 227:1-17, 1972) had done previously. Our results were similar to theirs: the diffraction lines became gradually clearer during contraction and were often spaced at intervals corresponding to sarcomere length differences of 40-45 nm. A cinematographic technique which recorded the entire diffraction pattern several times per second showed that there were some regions of the first order band in which the lines were not parallel; this may arise out of skewing of A and I bands along the muscle.

If our interpretation of the diffraction pattern holds, then the true molecular mechanism of contraction ought to include an inherent property which can predict discrete values of sarcomere length. The cross bridge theory does not appear to offer such a property.

F-AM-A3 IS MUSCLE FORCE INDEPENDENT OF SARCOMERE LENGTH BETWEEN 2 AND 3 μm? H.E.D.J. ter Keurs, T. Iwazumi and G.H. Pollack, Departments of Anesthesiology and Bioengineering, RN-10, University of Washington, Seattle, Wa. 98195

During tetanic contractions at long sarcomere lengths tension rises rapidly at first and then more slowly. It is the rapid rise component of tension that is used to construct the descending limb of the classical length-tension curve. The slow rise component has been ignored as it has been assumed to arise out of a gradually increasing dispersion of sarcomere lengths. We tested this assumption.

Sarcomere length and sarcomere length dispersion were measured on-line from laser diffraction patterns obtained from single fibers of frog semitendinosus muscle. Tetanic tension rose fast initially, then more slowly. A plateau was reached at a time which depended upon sarcomere length; it persisted for about 15 sec. Although sarcomere length changed during the period of increase of tension, it remained constant during the plateau. Sarcomere length dispersion at any position along the muscle was less than 1.2% of the mean sarcomere length at all times throughout the contraction. Thus we conclude that the assumption of increasing sarcomere length dispersion as the cause of the slow rise in tension is invalid. Therefore the premise upon which the descending limb of the classical length tension curve was obtained appears invalid.

We reevaluated the length tension relation by measuring tension and sarcomere length after the plateau of tension had been reached. In the sarcomere length range between 2.0 and 3.2 μm, plateau tension was length independent. The tension decreased to 80% of maximal tension between 3.2 and 3.4 μm and declined to zero at 3.65 μm.

Since tension and filament overlap are largely uncorrelated, it appears that a key argument supporting the cross-bridge theory is invalidated.

F-AM-A4 LIGHT DIFFRACTION STUDIES OF SARCOMERE DYNAMICS IN SINGLE SKELETAL MUSCLE FIBERS. P.J. Paolini, Dept. of Biology, San Diego State University, San Diego, CA 92182, K.P. Roos and R.J. Baskin, Dept. of Zoology, University of California, Davis, CA 95616.

A position sensitive optical diffractometer with better than 10 msec resolution has been used to examine the diffraction spectra produced by single skeletal muscle fibers during twitch and tetanic contraction. First order diffraction lines were computer analyzed for mean sarcomere length (from peak position), line intensity and percent dispersion in sarcomere length. Line intensity was observed to decrease rapidly by about 60% during a twitch, with an exponential recovery to resting intensity persisting well beyond cessation of sarcomere shortening (average time constant, 0.33 sec). Intensity recovery was particularly prolonged at zero filament overlap (e.g. at 3.8 u), with a recovery time constant of 1.47 sec. The occurrence of an intensity decrease at zero overlap suggests an origin other than force development per se, possibly activation, or actin-independent cross-bridge motion. A number of single fibers at initial lengths from 2.5 to 3.5 u exhibited a splitting of the first order line into two or more components during relaxation, with components refusing into a single peak by 200 msec after stimulation. This splitting reflects the asynchronous nature of myofibrillar relaxation within a single fiber. During tetanus, the dispersion decreased by more than 10% from onset (at 225 msec after stimulation) to plateau (at 2 sec), implying a gradual stabilization of sarcomeres. Dispersion during tetanic plateau increased linearly with sarcomere length.

F-AM-A5 SARCOMERE LENGTH-TENSION RELATION OF THE SINGLE CELL LAYERED HEART OF "SEA POTATO". L. Cleemann*, S. Dillon*, and M. Morad. Mt. Desert Island Biol. Lab. and Department of Physiology, Univ. of Pennsylvania School of Med., Philadelphia, Pennsylvania 19174.

Our previous studies have shown that the sea potato heart consists of a single layer of cells each containing a myofibril (2 - 4 μm in diameter) located near the luminal surface. The active and passive length tension relation of this heart was measured using a chamber in which the length of a small segment of the tissue was servo-controlled (J. Biophys. 16:208a, 1976). The speed of the servo-control system was increased as to clamp the length of the preparation within 5 - 10 msec. The sarcomere length was measured using diffracted light from a laser beam (3 m watts, HeNe, 636 nm). The light scattered by the muscle was focused on a linear array of 128 photodiodes (Reticon, RL128). In spite of small thickness of the myocardial sheath (8 - 10 μm), it was possible to measure the first order diffraction lines from the myofibrils when the beam was carefully collimated. The width of the diffraction line decreased as the preparation was stretched, suggesting an increase in the uniformity of sarcomere spacing. The diffraction line broadened and shifted by about 0.2 μm during an isometric twitch. The developed tension increased almost linearly as a function of sarcomere length between 0.7 - 2.2 μm. There was little or no resting tension in this range of sarcomere lengths. Attempts to stretch the myocardium beyond 2.2. μm led to rapidly developing resting tension, decreasing twitch tension and quick termination of the experiment. The maximum twitch tension is remarkably constant (0.8 kg/cm^2 assuming myofibrillar thickness of 3 μm) from preparation to preparation. These experiments showed that the contractile processes may be studied on the sarcomere level. The results are qualitatively similar to those found in vertebrate hearts. (HL 16152)

F-AM-A6 DEPOLARIZATION-INDUCED CALCIUM RELEASE FROM LIGHT AND HEAVY SARCOPLASMIC RETICULUM VESICLES. Kevin P. Campbell and Adil E. Shamoo, Dept. of Radiation Biology & Biophysics, The University of Rochester School of Medicine and Dentistry, Rochester, N.Y. 14642.

Light and heavy sarcoplasmic reticulum vesicles have been isolated from rabbit skeletal muscle using isopycnic zonal ultracentrifugation. In thin section electron microscopy the light sarcoplasmic reticulum vesicles (LSR) appear as empty vesicles whereas the heavy sarcoplasmic reticulum vesicles (HSR) appear as vesicles filled with electron dense material. SDS-gel electrophoresis showed that the LSR contains one protein, Ca^{2+}+Mg^{2+}-ATPase (~90%), and the HSR contains Ca^{2+}+Mg^{2+}-ATPase (~60%), calsequestrin (~25%), high affinity calcium binding protein (~5%) and several low molecular weight proteins. The biochemical and morphological data indicate that the LSR and the HSR are probably derived from the longitudinal and terminal regions of the SR, respectively. The LSR and HSR are both able to accumulate calcium in the presence of ATP to amounts greater than 100 nmoles of Ca/mg of membrane protein in less than one minute. Over 50% of the calcium accumulated by LSR and HSR can be released in less than 10 seconds by changing the anion outside the vesicles from methanesulfonate (MS) to chloride (Cl). Due to the difference in permeability between MS and Cl, this change should result in a decreased positivity inside the SR vesicles with respect to the exterior (or a 'depolarization' of the SR vesicles). A hyperpolarization (Cl to MS) causes no release of calcium. Na dantrolene (15μM)has no effect on LSR but inhibits slightly the release from HSR. The calcium specificity of the release is being investigated by passively loading the SR vesicles with Na-22 or C-14 sucrose and then depolarizing the vesicles.

Supported by US ERDA Contract and assigned report no. UR-3490-1021 and also supported by NIH and Muscular Dystrophy Association of America.

F-AM-A7 DIFFERENTIAL EFFECTS OF INTRACELLULAR ACID pH ON CA^{2+}-SENSITIVITY AND MAXIMUM FORCE GENERATION OF SLOW AND FAST TWITCH SKELETAL AND CARDIAC FIBERS OF RABBIT. S.K.B. Donaldson and L. Hermansen*, Departments of Physiology and Biophysics and Physiological Nursing, University of Washington, Seattle, Wash. 98195

The sarcolemmas of single slow (soleus) and fast (adductor) skeletal twitch fibers of rabbit were peeled off and small bundles of cardiac muscle with disrupted cell membranes were obtained via homogenization. The intracellular environment and Ca^{2+} activation of all fibers was controlled by varying bathing solution composition. Steady state isometric tension of (T) the fibers was measured using a photodiode transducer. Complete pCa vs. tension curves were collected at pH 7.0 and 6.5 (imidazole buffer) using identical bathing solutions for all fiber types and a paired data protocol. The following remained constant in every bathing solution: EGTA=7mM, $MgATP^{2-}$=2mM, μ=0.15M, K^{+}=70mM, Mg^{2+}=1mM, CP^{2-}=15mM, CPK=15 units/ml solution. Room temperature was 23±1°C and major anion was propionate. Ignoring differences in maximum tension by expressing T as percentage of maximum T at the same pH, the following 50% T points for the pCa-tension curves were determined:

	Soleus	Cardiac	Adductor
pCa for 50% T, pH7.0:	5.45	5.35	5.1
pCa for 50% T, pH6.5:	5.25	4.9	4.85

Also, the absolute maximum tension declined at pH6.5 such that mean Tmax (pH 6.5)/Tmax (pH7.0) was 0.88 for soleus, 0.78 for cardiac, and 0.70 for adductor. All effects of lowering pH to 6.5 were reversible. In considering the combined effects of pH6.5 on Ca^{2+}-sensitivity and absolute magnitude of force generation, it is apparent that cardiac muscle force generation is more greatly depressed by acidosis than that of skeletal muscle; and adductor is more sensitive to acidosis than soleus muscle. Research supported by USPHS grants HL17373, RR00374 from NIH.

F-AM-A8 REGULATION OF Ca^{++} EFFLUX FROM THE SR BY ATP, Mg^{++} AND Pi IN THE ABSENCE OF SUBSTRATE IN SKINNED MAMMALIAN SKELETAL MUSCLE. Donald S. Wood*, David A. Kahn*, Sharon Selinger* and John P. Reuben, H. Houston Merritt Research Center, Dept. Neurology, Columbia University, New York, New York 10032.

The rate at which Ca^{++} is lost from the SR in the absence of substrate (Ca-pump turned off) was tested in chemically skinned rabbit psoas fibers. The SR was loaded by exposing the fiber to standard Ca^{++} saline: $10^{-6.4}$ M Ca^{++}, 2 mM MgATP (pH 7.0, γ = 200 mM). The fiber was then exposed to a Ca-efflux solution (substrate-free, 5-10 mM EGTA, Ca < 10^{-9} M) for up to 7 min. After the efflux period the SR was challenged with a standard caffeine (10-20 mM) saline containing 2.0 mM substrate, thereby allowing the caffeine-released Ca^{++} to be monitored by means of a tension. Varying the period for Ca^{++} efflux into a substrate-free solution from 0 to 7 min produced little change in the caffeine-releasable Ca, i.e., the tension amplitudes diminished less than 30%. Addition of ATP (0.1-0.5 mM) to the efflux solution accelerated Ca^{++}-loss; tension was abolished after 3 min exposure to 0.5 mM ATP. Mg (1.0-10 mM) decreased the loss, while Pi (2 mM) had no effect. Unexpectedly an equimolar combination of Mg with Pi (0.5-0.8 mM) also stimulated Ca^{++} loss from the SR. Thus, Ca^{++} efflux can be strongly influenced by ATP, Mg and the combination of Mg^{++} with Pi independently of effects these ions may have on the rate of active Ca^{++} accumulation by the Ca^{++} pump. Supported in part by MDAA and N.I.H.

F-AM-A9 ^{45}Ca RELEASE IN SKINNED MUSCLE FIBERS STIMULATED AT MODERATE (Mg^{++}). E. W. Stephenson, NIAMDD, NIH, Bethesda, Maryland 20014

The response of skinned muscle fibers to a Cl stimulus at 19°C depends on both the applied Cl gradient and (Mg^{++})(Stephenson & Podolsky, Fed. Proc. (1974) 33:1260). With a small gradient, substantial responses occur only at very low Mg^{++} (20 μM), and ^{45}Ca release from the sarcoplasmic reticulum (SR) is inhibited by EGTA (ethyleneglycol-bis(aminoethylether)N-N' tetraacetic acid)(Stephenson, Physiologist (1975) 18:407). Thus Ca release appears to be Ca-dependent under those conditions. In the present work, the time course of ^{45}Ca loss and the effect of EGTA were studied during responses to a larger Cl gradient at 110 μM Mg^{++}; this (Mg^{++}) inhibits force transients induced by an external Ca stimulus. Segments of skinned fibers from frog semitendinosus muscle were loaded with ^{45}Ca and stimulated by Cl at 19°C while isometric tension and ^{45}Ca loss to the bath were followed simultaneously. Force approached peak value within 2 sec and had decayed within ~ 10 sec. Response size varied, but initial force development and ^{45}Ca loss were well correlated. Myofilament space (MFS) ^{45}Ca was chelated by EGTA applied either 1) after the force transient was completed, 2) near the peak of the force transient, or 3) preceding or with the Cl. The main findings were: a) The initial net ^{45}Ca efflux to the bath was > 100 times efflux after relaxation; b) About 70% of the ^{45}Ca estimated to be in the MFS at the force peak was reaccumulated by the SR in ~ 4 sec; c) In the presence of MFS EGTA, stimulation of ^{45}Ca release was strongly inhibited; a small transient increase in efflux, insufficient to produce force, was detectable. These results suggest that 1) at moderate (Mg^{++}), depolarization induces rapid Ca release which is highly Ca-dependent; 2) the released Ca is rapidly reaccumulated.

F-AM-A10 EFFECTS OF HALOTHANE ON TENSION AND CALCIUM RELEASE IN MECHANICALLY SKINNED PORCINE SKELETAL MUSCLE: STUDIES ON MALIGNANT HYPERTHERMIA. R.E. Godt and M.J. Hahn, Department of Pharmacology, Mayo Foundation, Rochester, MN. 55901.

Anesthetic-induced malignant hyperthermia is thought to be due to action of anesthetic on skeletal muscle. To study this, skinned muscle fibers from semitendinosus of Poland China pigs, either resistant (MHR) or susceptible (MHS) to halothane-induced malignant hyperthermia, were placed in solutions with (in mM) 2 MgATP, 0.5 Mg^{2+}, 14.5 creatine phosphate, 20 imidazole, 48 K propionate, 7 EGTA with varying $CaCl_2$; ionic strength was 0.15, pH 7.0, and temperature 37°C. Striation spacing was set to 2.6μm. Halothane at 2% was bubbled into the solution and measured with gas chromatography. Without halothane, maximal tension at pCa 4 was 20% lower in MHS muscle. Halothane decreased maximal tension by 16% in both MHR and MHS muscle. We used caffeine and change of anion from propionate to chloride to release calcium from sarcoplasmic reticulum of fibers loaded with calcium at pCa 6.25. Release was estimated from peak values of tension. Loading appeared to be unaffected by halothane. With halothane, more caffeine is required for release in both MHR and MHS muscle. Anion-induced release from MHS muscle was not always antagonized in MHR muscle. In summary, decrease calcium-activated tension in both types of muscle but its effect on submaximal tension in MHS muscle is greater than on MHR muscle. Its antagonism of calcium release induced by anion exchange is more profound in MHS muscle. (Supported by Muscular Dystrophy Assoc. grant MDA-15 and PHS grant AM 17828)

pCa	6	5.75	5.5	4
	NORMALIZED TENSION(%)			
MHR control	0	24	77	100
+halothane	0	10	89	100
MHS control	5	58	76	100
+halothane	2	40*	83	100

(*significant change from control)

F-AM-A11 THE EFFECTS OF HALOTHANE ON Ca^{2+} -ACTIVATED TENSION DEVELOPMENT OF SKINNED RABBIT PAPILLARY MUSCLE FIBERS. J. Y. Su and W. G. L. Kerrick, Department of Anesthesiology and Department of Physiology and Biophysics, University of Washington, Seattle, WA 98195.

We investigated the halothane-induced myocardial depression on Ca^{2+}-activated tension development of skinned rabbit right ventricular papillary muscle fibers. Fiber bundles (≈100μ dia.) were isolated from homogenized muscle and mounted in a tension transducer at resting sarcomere length of approximate 2.1μ. The experimental solutions contained [Mg^{2+}] =1, [K^+] =70, [$MgATP^{2-}$]=2, [CP^{2-}]=15, [EGTA] total =7(in mM), [Ca^{2+}] at various concentrations (pCa=3.8, 5.0, 5.2, 5.4, 5.6, or >9) and [imidazole propionate] adjusted to maintain ionic strength=0.15 and to control pH=7.00±0.02 at 21°C. Each fiber was immersed in control solutions equilibrated with 100% N_2 and test solutions equilibrated with halothane and N_2. Halothane concentrations of the solutions were assayed by gas chromatography.

The halothane effect on the maximum Ca^{2+}-activated tension (pCa=3.8) is shown in the following dose-response relationship (mean ± SE(n), *=p< 0.001 compared to control by paired t test):

Halothane (%)	% of control	Halothane	% of control
1	93±1(16)*	3	80±1(32)*
2	85±1(20)*	4	76±1(18)*

In contrast to the maximum response at pCa=3.8, tension (%) at submaximum [Ca^{2+}] (pCa = 5.0 to 5.6) relative to the maximum tension was not depressed by halothane at concentrations less than 2%. It is concluded that halothane, at clinical concentrations, directly depressed the interactions of the contractile proteins and, to a lesser degree the regulatory proteins. The halothane-induced depression was reversible. Supported by grants from NIH-GM15991, GM01160 and AM17081 and American Heart Association.

F-AM-A12 THE ENERGY BALANCE OF CROSSBRIDGE CYCLING IN FROG SKELETAL MUSCLE. C. Kean*, E. Homsher and V. Sarian-Garibian*. Dept. of Physiology, U.C.L.A., Los Angeles, CA 90024.

Phosphocreatine (PC) hydrolysis is the only net reaction known to occur during muscle contraction, yet less than 0.75 of the energy produced during isometric tetani can be accounted for by PC splitting. Furthermore, this fraction (the explained enthalpy fraction (EEF), which is the product of the measured PC splitting and the molar enthalpy change for PC hydrolysis (-34 kJ/mol) divided by the observed energy liberation) declines to only 0.5 in tetani in which thick and thin filament interaction is abolished by setting the sarcomere spacing to 3.6μm (The Physiologist (1976) 19: 250). These results suggest that calcium release and sequestration may involve unidentified exothermic reaction(s), while the crossbridges may cycle with an EEF of 1.0. To test this idea, pairs of semitendinosus muscles were tetanized for 5 s at 0°C under isometric conditions, with one of the muscles at a sarcomere length of 3.6μm, the other at 2.0 - 2.2μm, and the differences in PC splitting and heat production were measured. The shorter muscle should produce energy and split PC associated with crossbridge cycling, calcium release and sequestration while only the latter processes with associated energy production and PC splitting should occur in the stretched muscle; the difference should reflect crossbridge activity alone. The difference in heat production was 1.01 ± 0.05 mJ/μmol total creatine (CT) (mean ± S.E.M., n=6) while the net PC hydrolysis was 29.5 ± 2.1nmol PC/μmol CT (mean ± S.E.M., n=13). Thus PC splitting accounts for 1.00 mJ/μmol CT and the EEF is 0.99. This experiment indicates that the energy liberation associated with crossbridge cycling can be fully accounted for by PC splitting and that the lack of energy balance in isometric tetani stems from unidentified reaction(s) associated with calcium release and reuptake. Supported by USPHS grant # HL 11351 and AHA-GLAA grant # 525)

F-AM-A13 DETERMINATION OF PHOSPHATE UTILIZATION IN INTACT MUSCLE BY ^{31}P NMR. C.T. Burt, R. Labotka*, J. Flaherty*, M. Danon*, T. Glonek* and M. Bárány. University of Illinois at the Medical Center, Chicago, Illinois 60612

Changes in the phosphate metabolites, including high energy phosphates of muscle, were, in the past, routinely determined by perchloric acid extraction and subsequent chemical analysis. Now it is possible to follow such changes in the intact muscle by ^{31}P NMR (Burt, et al., J. Biol. Chem., 251, 2584, 1976 and Dawson, et al., J. Physiol., 258, 82P, 1976). Furthermore, the analysis of enzyme activity in the same sample of intact muscle would be difficult to determine except by NMR. We have analyzed the anaerobic behavior of frog gastrocnemius muscle and found that the rate of disappearance of phosphocreatine (PCr) or appearance of inorganic phosphate (P_i) yields a resting heat at 28°C of 1.5 mcal/gm/min which compares well with that calculated from the resting heat at 20°C, 1 mcal/gm/min using a Q_{10} of 2. If all the ATPase is generated by actomyosin, one would have an activity of 1.5 nanomoles P_i/mg protein/min and a rate constant of 1.23×10^{-4} sec^{-1} with a half life of ATP of 94 min. Data from human muscle shows such analysis can be useful in the characterization of diseased states. As an example, the ratio of $(dP_i/dt)/-(dPCr/dt)$ is greater than 1.5 in both a gastrocnemius affected by Duchenne dystrophy and a quadriceps affected by nemaline rod myopathy while it is 1.2 for a normal quadriceps and 1.4 for a normal pectoralis. Treatment of frog gastocnemius with 20 mM caffeine accelerates the usage of PCr by a factor of about 6 to a value of 1.0 micromoles PCr/gm/min. The ratio of PCr usage to the tension time integral (determined independently) was 0.02 micromoles PCr/gm/min. This ratio of PCr usage to tension time implies other energy yielding reactions. (Supported by a grant from the Chicago Heart Association, MDA, MDAC, and NIH grants GRS-7544 and NS-12172).

F-AM-A14 RELATIONSHIP BETWEEN INITIAL CREATINE PHOSPHATE (CP) BREAKDOWN AND RECOVERY OXYGEN CONSUMPTION FOR SINGLE ISOMETRIC TETANI OF THE FROG SARTORIUS AT 20°C. M. Mahler* (Intr. by W. Mommaerts). Department of Physiology, UCLA, Los Angeles, CA 90024.

Previously, we described the time course of the suprabasal rate of oxygen consumption (ΔQ_{O_2}) in the sartorius of R. pipiens after isometric tetani of 0.1 - 1.0 sec at 20°C (Mahler, Fed. Proc. 35: 290, 1976). To test for the existence of post-contractile CP splitting, the CP breakdown during a tetanus ($\Delta[CP]_o$) was compared with the total suprabasal oxygen consumption during recovery ($\Delta[O_2]$), measured as the integral of $\Delta Q_{O_2}(t)$. If post-contractile splitting is negligible in comparison with that during a tetanus, the ratio $\Delta[CP]_o/\Delta[O_2]$ should closely match the in vivo P:O_2 ratio, which has an expected value of 6.2 - 6.5. The results are as follows (mean±SEM (n)):

Tetanus duration (sec)	0.2	0.5	1.0
$\Delta[CP]_o$ (μmole/g)	1.44±0.25 (11)	2.98±0.30 (9)	4.31±0.24 (15)
$\Delta[O_2]$ (μmole/g)	0.20±0.02 (12)	0.41±0.04 (7)	0.65±0.03 (8)
$\frac{\Delta[CP]_o/(P_{max}\ell_o/C_T)}{\Delta[O_2]/(P_{max}\ell_o/C_T)}$	6.32	6.50	6.21

These results imply that in the frog sartorius at 20°C:(a) the in vivo P:O_2 ratio matches the in vitro value;(b) for tetani of 0.2 - 1.0 sec, suprabasal CP splitting during recovery is very small in comparison with that during a tetanus; and (c) the reversal of unidentified exothermic reactions occurring during a tetanus (Woledge, Prog. Biophys. 22: 39-74, 1971) must be coupled to negligible CP splitting. (USPHS Grant# HL 05696)

F-AM-A15 ISOLATION OF PHOSPHORYLATED ACID CHLOROFORM-METHANOL SOLUBLE PROTEINS FROM LIVE FROG MUSCLE. M. Bárány, K. Bárány, E. Gaetjens, and A. Steinschneider*, Departments of Biological Chemistry and Physiology, University of Illinois at the Medical Center, Chicago, Illinois 60612

About 6-7% of the total proteins from trichloroacetic acid washed and freeze-dried frog muscle could be extracted with acid chloroform-methanol. When these proteins were extracted from muscles of frogs, which were injected with ^{32}P orthophosphate and left at room temperature for 1 to 2 days, a part of the proteins was found to be labeled. As a first step for their isolation, the proteins were separated from lipids by gel filtration on Sephadex LH-20 in acid chloroform-methanol. After evaporating the solvent the proteins were dissolved in 0.1% SDS, 8.0 M urea, and 0.1 M sodium phosphate buffer, pH 7.0, and purified in this solvent by preparative gel electrophoresis. The radioactive proteins were eluted and were found to migrate as a single band upon repeated electrophoresis. Three phospho-proteins were prepared by this procedure with apparent molecular weights of 34,000, 19,000 and 10,000, determined by SDS-gel electrophoresis. These three phosphoproteins were different as indicated by their amino acid composition. Surprisingly, the content of their hydrophobic residues was only 19-28% of the total amino acids. Furthermore, the purified proteins did not contain significant amount of tightly bound neutral- or phospholipids in spite of their solubility in acid chloroform-methanol. The 10,000 dalton protein, which had the highest specific radioactivity, contained an unusually high proportion of serine, 14% of the total amino acids. It also did not stain with Coomassie Blue. All three proteins incorporated ^{32}P exclusively into serine phosphate, and each phosphorylated protein contained 3 moles of a covalently bound neutral sugar. (Supported by NS-12172 from NIH, MDA, and MDAC).

F-AM-A16 OPTIMAL LEVEL OF CREATINE PHOSPHATE IN MAXIMALLY-ACTIVATED GUINEA PIG VENTRICULAR BUNDLES. D.W. Maughan, E.S. Low* & N.R. Alpert. Dept. of Physiology & Biophysics, Univ. of Vermont, Burlington, VT 05401

We have used mechanically disrupted heart fragments (Kerrick & Best, Science, 183, 435-437, 1974) for studying muscle mechanics, since Ca^{2+} activation can be controlled while muscle force and velocity are measured. A creatine phosphate (CP) and creatine phosphokinase (CPK) ATP regenerating system is used so that intracellular MgATP is effectively maintained. In the absence of a regenerating system, rigor complexes formed in the bundle core during contraction are likely to increase tension and retard muscle shortening rate. We determined an optimal level of CP in ventricular bundles (0.1-0.2 mm dia) at pMgATP=2.7, pMg=3.3, pH=7.0, ionic strength=0.15 M and CPK=1 mg/ml; pCa=9.0 (relaxing solution) and 4.0 (maximal activating solution). The effect on tension and velocity of adding CP is shown in the table below. Force measurements, P_o, were taken after the Ca^{2+}-activated tension reached a plateau; velocity, V, immediately following a quick release to a relative load $P/P_o=0.2$. Muscles were stretched by 20% in order to compensate for internal shortening during activation preceding release (estimated to be 15-25% from an analysis of the elastic recoil). At 15 mM CP, mean P_o was 0.81 ± 0.32 (SD) kg/cm^2; mean V was 0.36 ± 0.11 muscle lengths/sec. Irreversible changes in P_o and V occurred in low CP (0-5 mM) solutions. 10-15 mM CP appears to be sufficient to maintain intracellular MgATP levels during maximal Ca^{2+} activation.

Supported by Vt. Heart Assoc. grant 5-26531.

Table: Effect of [CP] on isometric force and isotonic velocity ($P/P_o=0.2$) at 22°C.

[CP], mM	0	5	10	15	25	
Force, %	151±16	128±15	100±2	100	96±4	(Average±SD)
Velocity, %	71±13	80±14	99±9	100	87±7	

F-AM-A17 IONIZED MAGNESIUM CONCENTRATION IN BARNACLE MUSCLE FIBERS. Teresa Tiffert, F. J. Brinley, Jr., and A. Scarpa, Dept. of Physiology, University of Maryland School of Medicine, Baltimore, Md. 21201 and Dept. of Biochemistry and Biophysics, University of Pennsylvania School of Medicine, Philadelphia, Pa. 19104.

Intracellular ionized Mg was determined in single isolated barnacle muscle fibers by injecting Eriochrome Blue SE, a Mg indicator, into the fibers and measuring the differential absorbance change of the Mg-EB complex when the concentration of cytoplasmic Mg is perturbed by internal dialysis of the fiber (using a porous plastic capillary 140μ O.D.) with an isotonic mixture of 250 mM EGTA + 80 mM KTES containing varying amounts of Mg (0-80 mM). Absorbance changes were measured by means of multichannel microspectrophotometry. Three wavelengths were monitored simultaneously, the pair 580 - 550 nm, insensitive to calcium and the isosbestic point at 566 nm. When the free Mg concentration in the dialysis solution is the same as that in the cytoplasm, dialysis does not change the internal Mg concentration and therefore produces no change in the differential spectrum of the dye in the sarcoplasm. Mismatch in the free Mg concentrations of dialysate and cytoplasm is reflected as a change in differential absorbance. Calibration of free Mg in dialysis solutions was done by dialyzing a 1 mm diam. glass capillary containing a solution of artificial sarcoplasm and Eriochrome Blue SE with added known amounts of total Mg. Results indicated that the free ionized Mg is about 4.2 mmole/kg wet wt or 6 mM in the intracellular water immediately surrounding the dialysis capillary. The ATP concentration was estimated to be 4.9 mmole/kg wet wt by using the firefly method. Partitioning of Mg among various intracellular constituents based on present data combined with published work by others is (mmole/kg wet wt): free, 4.2; MgATP, 4.2; myofibrillar bound, 1; residual (presumably bound to amino acids and phosphate) ca. 1. Supported by NIH Grants NS-08336, HL-18708 & 7 F22NS00021-03.

F-AM-B1 INTERACTION BETWEEN A LOCAL ANESTHETIC, THE SODIUM CHANNEL GATES AND TETRODOTOXIN (TTX). W. Almers and M. D. Cahalan, MBL Woods Hole, MA, and Depts. of Physiology, U. of Washington, Seattle, WA 98195 and U. of Pennsylvania, Philadelphia, PA 19174.

We have studied effects of the quaternary lidocaine derivative QX-314 (QX) on gating and sodium currents (I_{Na}) of internally perfused, voltage-clamped squid giant axons. As in frog nerve (Strichartz, JGP 62:37; Courtney, JPET 195:225) block of sodium channels by internally applied 1 mM QX is strongly enhanced if a train of conditioning depolarizations precedes the measurement ("use-dependent block"), possibly because sodium channels must open before QX can enter and block them. Extent of block depends on the potential during conditioning pulses in a manner expected either if Na^+ could knock QX off its blocking site, or if QX has to cross 95% of the membrane electric field before reaching this site. When sodium channel inactivation is abolished by pronase, conditioning depolarizations no longer enhance block significantly. This suggests that use-dependent block in normal axons may occur because the "inactivation gate" hinders exit of QX from its blocking site. QX-block in pronase-treated axons is time-dependent, appearing as a QX-induced inactivation of sodium conductance under a 20 msec depolarization. Sodium channel gating currents in normal axons are measurably reduced by QX only if a train of conditioning depolarizations precedes the measurement. Conditioning pulses producing 90% block of I_{Na} by QX result in nearly twofold reduction in total gating charge movement. In the presence of external TTX (4×10^{-7}M) and internal QX, gating currents are always about half their normal size regardless of conditioning, as if QX were then permanently present in the channel. Perhaps TTX promotes QX-induced block of gating currents by protecting the QX bound in the channel against being knocked away by sodium ions. (Supported by USPHS grants AM-17803 and NS-08951)

F-AM-B2 ACTION MODE OF LOCAL ANESTHETICS ON AXON MEMBRANE EXCITABILITY. S. Ohki and C. Gravis*, Dept. of Biophysical Sciences, State University of New York at Buffalo, N.Y. 14226 and Y. Shinagawa, Dept. of Physiology, Kyoto University, Kyoto, Japan.

A study was made on action mode of tertiary amine local anesthetics on lobster axon excitability. The experiments were to measure a minimum concentration of extracellularly applied local anesthetics to exert a narcotic action on the axon membrane, and the time to exert a narcotic action after application of a given concentration of a local anesthetic to the extracellular solution. A theoretical relationship for an action mode was obtained in terms of the internal and external pH's, the external concentration of local anesthetics, its permeability across the membrane and the time to exert the narcotic action. The experimental data were analyzed in comparison with the theoretical formulation for the action mode. It is deduced that the action mode of tertiary amine local anesthetics is, first to penetrate into the axon interior in a neutral form, and then to react in a cationic form electrostatically from the intracellular phase and, finally, to exert narcotic action by hydrophobic interaction.

In addition, permeabilities of the neutral form of local anesthetics were obtained for each local anesthetic at different pH, and they are compared with the results obtained by the isotope tracer method (Dettbarn et al., Neuropharmacology 11:727 (1972)) for the uptake of local anesthetics into the axon interior.

F-AM-B3 MECHANISM OF BLOCKAGE OF SODIUM CHANNELS BY YOHIMBINE IN SQUID GIANT AXON. R.J. Lipicky, G. Ehrenstein, and D.L. Gilbert, Dept. Pharmacology, College of Medicine, University of Cincinnati, Cincinnati, Ohio 45267; Laboratory of Biophysics, NINCDS, National Institutes of Health, Bethesda, Maryland 20014, and Marine Biological Laboratory, Woods Hole, Mass. 02543

The effects of yohimbine, an alkaloid, alpha adrenergic blocking agent, are very similar to the effects of local anesthetics. In particular, yohimbine causes use-dependent inhibition of sodium channels in the squid giant axon. We have studied this effect by applying a time series of depolarizing voltage clamp pulses in the presence of yohimbine, and determining the final blockage of the sodium currents. Experiments were performed at various pulse amplitudes, various pulse widths, and with and without pronase treatement. We found that final blockage is a sigmoidal function of pulse width, with saturation at about 1 millisecond. The fact that longer pulses are not more effective at blocking channels indicates that the voltage pulses induce blockage by opening the channels. Although the magnitude of the current decreased during successive pulses, there was no change in the shape of the current-time records, indicating that the blockage occurs between depolarizing pulses. This delay between yohimbine binding and blockage argues that yohimbine blocks sodium channels by keeping the sodium gates closed, rather than by occluding the channels. Support for this conclusion was obtained from experiments with pronase, which indicate that after pronase treatment, channels cannot be blocked by yohimbine.

F-AM-B4 EFFECT OF TEMPERATURE ON TETRODOTOXIN ACTION AND MEMBRANE CAPACITANCE IN SQUID *DORYTEUTHIS PLEI*. C. Sevcik. Centro de Biofísica y Bioquímica, Instituto Venezolano de Investigaciones Científicas (IVIC), Caracas 101, Venezuela.

Previous work of our lab indicates that in *D. plei* at 21°C, tetrodotoxin interacts with two types of receptors. We have analyzed the effect of temperature on TTX action in *D. plei* axons under potential control and found that the two receptors may be evidenced at over 15° C. Below this temperature, only one kind may be identified. The affinity constants (K_1 and K_2) and the proportions ($Ymax_1$ and $Ymax_2$) of each type are at: *30°C*, K_1 = 25.0 ± 8.0 pM, K_2 = 6.09 ± 1.19 nM, $Ymax_1$ = 22.2 ± 2.3%, $Ymax_2$ = 83.8 ± 2.5%; *25°C*, K_1 = 54.0 ± 11.0 pM, K_2 = 15.1 ± 2.7 nM, $Ymax_1$ = 23.6 ± 6.3%, $Ymax_2$ = 76.3 ± 6.3%; *21°C*, K_1 = 0.11 ± 0.05 nM, K_2 = 4.9 ± 0.5 nM, $Ymax_1$ = 19.0 ± 4.7%, $Ymax_2$ = 84.0 ± 4.1%; *15°C*, K_1 = 0.17 ± 0.06 nM, K_2 = 1.7 ± 0.3 nM, $Ymax_1$ = 35.8 ± 8.9%, $Ymax_2$ = 63.3 ± 9.0%; *10°C*, K_1 = 0.67 ± 0.06 nM, $Ymax_1$ = 101.2 ± 2.1%; and *5°C*, K_1 = 0.94 ± 0.23 nM, $Ymax_1$ = 93.9 ± 2.9%. When membrane capacitance is measured with ramps of 100 volt/sec, two different values are obtained: ≃1.04 μF/cm^2 between 5 and 10°C, and ≃1.22 μF/cm^2 for 15 to 30°C. A constant value of ≃1.00 μF/cm^2 is obtained in the range from 5 to 30°C with ramps of 1600 volt/sec. The peak inward sodium current decreases from ≃8 mA/cm^2 to ≃2 mA/cm^2 when the nerves are cooled from 20 to 5°C. The changes in low frequency membrane capacitance with temperature, and the independence from it of the high frequency capacitance, suggests that the mobility of membrane macromolecules, probably proteins (Takashima, Yantorno and Pal, 1975), decreases between 10 and 15°C, this decrease may reflect less freedom to change between different conformations and may be responsible for the diminished sodium current and the lack of low affinity receptors for TTX below 15°C. (Supported in part by CONICIT, Venezuela, Grant N°31.26.S1-0590.

F-AM-B5 MODIFICATIONS OF IONIC CONDUCTANCES IN SQUID AXON PRODUCED BY THE DIPOLAR FORM OF PHLORETIN. G.S.Oxford, F.Ramon, & G.R.Strichartz, Dept. of Physiology, Univ. of No.Carolina, Chapel Hill, N.C. 27514, Dept. of Physiology and Pharmacology, Duke Univ.,Durham, N.C.27710, & Dept. of Physiology and Biophysics, SUNY, Stony Brook, N.Y. 11794 & the Marine Biological Laboratory, Woods Hole, MA. 02543.

Phloretin reversibly modifies the sodium and potassium conductances of squid axons. The maximum sodium conductance, $\bar{g}_{Na}$, is reduced to 70% of control and the membrane potential to activate 0.2 of the remaining conductance ($V_m0.2$) becomes 12mV more depolarized than control with internal phloretin ($5x10^{-5}$M,pH_{in}7.3). Both g_{Na} depression and the shift of $V_m0.2$ are greater at internal pH 6.2 than pH 8.7, evidence that the unionized form of weakly acidic phloretin (pK_a7.3) is the more effective form. External phloretin produces similar effects. Neither the time-to-peak I_{Na} nor the sodium inactivation are significantly changed by phloretin. Potassium conductance is modified by internal phloretin ($5x10^{-5}$M,pH_{in}7.3) in three ways: 1) maximum $g_K(\bar{g}_K)$ is reduced (47% of control) 2) V_m 0.2 of the remaining g_K is shifted to more depolarized potentials (≃31mV) and 3) the time-course of g_K is slowed, with half-times at least doubled. Again, these effects are larger ($\bar{g}_K/\bar{g}_K$ control=21%;$\Delta V_m0.2$= 44mV) at internal pH 6.2, indicating greater effectiveness of the unionized form. In addition, the slope of the g_K vs E_m relation (10 fold/22mV, control) was decreased by $5x10^{-5}$M internal phloretin at pH 6.2 (10 fold/32mV), a change not seen with phloretin at pH 8.7. Unionized phloretin may act at the inner surface of the membrane to change the gating of potassium channels by producing a local dipole field in the membrane, as has been reported for phospholipid bilayer membranes.

F-AM-B6 DEOXYCHOLATE BINDS TO THE SODIUM CHANNEL IN RESTING STATE. Chau H. Wu, Paul J. Sides,* and Toshio Narahashi, Department of Physiology and Pharmacology and Department of Pathology, Duke University Medical Center, Durham, North Carolina 27710

Sodium channels in squid axon membranes treated with deoxycholate (DOC) exhibited two types of conductance kinetics, i.e. a fast transient component and a slowly activating but non-inactivating component. The coexistence of the two types of Na channel could be observed in high DOC concentrations or after the sodium inactivation had been removed by internal treatment with 1 mM N-bromoacetamide. The fast transient component could be eliminated by lowering the temperature or applying depolarizing prepulses so that only the slow persistent component remained. The relative proportion of the two components was a function of DOC concentration and temperature. The voltage dependence, reversal potential, and kinetics of the tail current of the two components were not greatly different. Both types of channel could be blocked by external application of tetrodotoxin or internal application of pancuronium. These observations can be explained by the binding of DOC to the Na channel in resting state. Depolarization of the membrane perturbs the equilibrium of the reversible binding and results in a slow release of m gate to allow it to undergo activation. The tight binding of the negatively charged carboxylic end to the h gate accounts for the failure of inactivation for a moderately long period of time. Thus the action of DOC demonstrates that the activation and inactivation gates are separable. Supported by NIH Grant NS10823.

F-AM-B7 VOLTAGE DEPENDENCE OF CATION PERMEABILITY RATIOS IN SQUID AXON MEMBRANES. I. Seyama,* and T. Narahashi, Department of Physiology and Pharmacology, Duke University Medical Center, Durham, North Carolina 27710

Resting squid axon membrane exhibits a poor selective permeability to various organic and inorganic cations (Hironaka and Narahashi, Fed. Proc. 34, 360, 1975). This is in sharp contrast with the situation during activity when the membrane becomes highly selective. However, since the cation permeability ratios at rest and during activity were measured at different membrane potential levels, a question remains as to whether the difference in permselectivity is due to a voltage dependence of permeability ratio. To clarify this point, the cation permeability ratios were measured as a function of the membrane potential. Permeability ratio (P_X/P_{Na}) was calculated at various membrane potentials from the reversal potential for peak transient current. The logarithm of P_X/P_{Na} is linearly related to the membrane potential, increasing with hyperpolarization. The P_X/P_{Na} ratios for hydroxylamine, formamidine, ammonium, and guanidine are moderately voltage dependent, whereas those for methylguanidine, cesium, methylamine, and choline are highly voltage dependent. For example, the P_X/P_{Na} ratio for formamidine is 0.13 at +40 mV and increases to 0.51 at -70 mV as estimated by extrapolation. The ratio for methylguanidine is 0.05 at -20 mV and increases to 1.2 at -70 mV. The permeability ratio of the resting membrane, as measured by voltage clamp also increases with hyperpolarization. Thus it can be concluded that the difference in cation permselectivity at rest and during activity is at least in part due to the voltage dependent nature of the permeability ratio. Supported by NIH Grant NS10823.

F-AM-B8 PANCURONIUM BLOCK OF Na CHANNELS OF SQUID AXON MEMBRANES TREATED WITH PRONASE OR N-BROMOACETAMIDE. J. Z. Yeh, and T. Narahashi, Department of Physiology and Pharmacology, Duke University Medical Center, Durham, North Carolina 27710

Pronase and N-bromoacetamide (NBA) are known to remove Na inactivation when perfused internally to squid axons (Armstrong et al., J. Gen. Physiol. 62, 375, 1973; Oxford et al., Biophys. J. 16, 187a, 1976). Direct interactions of blocking agents with Na channels can be studied with these preparations without complications from the Na inactivation. Pancuronium has been shown to block the Na channel of pronase-treated axons in a time-dependent manner (Yeh and Narahashi, Biophys. J. 15, 263a, 1975). The pancuronium-induced block follows a single exponential time course, and the time constant depends upon the axoplasmic concentration of pancuronium, being shorter for higher pancuronium concentrations. The reciprocal of time constant measured at 80 mV is a linear function of pancuronium concentration (0.1-1 mM). Pancuronium exhibits a similar block of Na channel of NBA-treated axons, but the time constants of block are 2 to 3 times longer than those measured in pronase-treated axons at the corresponding pancuronium concentrations. The activation mechanism (m^3 gate) of Na channel is not affected by either pronase or NBA treatment. The difference in the time course of pancuronium block suggests that pronase and NBA modify the Na channel pore in different manners. These results support the notion that an additional positive charge brought to the Na channel by NBA causes a decrease in pancuronium concentration near the inner mouth of the channel thereby decreasing the rate of block. Supported by NIH Grant NS10823.

F-AM-B9 OBSERVATIONS ON SODIUM CHANNEL ACTIVATION GATING IN SQUID AXONS INTERNALLY PERFUSED WITH PRONASE OR N-BROMOACETAMIDE. G.S. Oxford and J.Z. Yeh, Department of Physiology, University of North Carolina, Chapel Hill, N.C. 27514 and Department of Physiology and Pharmacology, Duke University Medical Center, Durham, N.C. 27710.

The gating behavior of sodium channels in squid axon membrane was examined before and after removal of normal sodium inactivation by treatment with either Pronase or N-Bromoacetamide (NBA) (Armstrong et al. 1973. J. Gen. Physiol. 62:375; Oxford et al. 1976. Biophys. J. 16:187a). Sodium currents were measured in axons internally perfused with 275 mM CsF substituted for K^+ and bathed in low external sodium. The m_∞ -voltage relation of the Hodgkin-Huxley model measured from analysis of steady-state I_{Na} after Pronase or NBA treatment did not differ significantly from measurements from standard analysis of normal sodium currents. Kinetics of activation (τ_m) were not significantly changed following Pronase treatment. Comparison of τ_m values obtained from the turn-on of I_{Na} with time constants for the decay of sodium tail currents at overlapping voltages showed reasonable agreement, however, τ_m values derived from tail currents were greater than expected from the Hodgkin-Huxley formulation. Activation kinetics were found to be independent of the direction of ion movement in a few experiments where the direction of I_{Na} at a given voltage was reversed by changing the external sodium. Changes in the shape of sodium activation kinetics were observed with test depolarizations applied at various intervals during the decay of sodium tail currents. These observations are consistent with the notion that activation and deactivation of sodium conductance involves transitions of a sequential multistate nature. Supported by N.I.H. grant NS10823 to Dr. T. Narahashi.

F-AM-B10 INTERACTION BETWEEN BATRACHOTOXIN AND YOHIMBINE IN CULTURED NEUROBLASTOMA CELLS. L.M. Huang, G. Ehrenstein, and W.A. Catterall*, Laboratory of Biophysics, NINCDS and Laboratory of Biochemical Genetics, NHLB, National Institutes of Health, Bethesda, Md., 20014

Batrachotoxin, a specific activator of sodium channels, can cause as much as 25-fold increase in the rate of Na^+ uptake in neuroblastoma cells. This batrachotoxin-induced Na^+ uptake provides a means of measuring the passive steady state Na^+ permeability associated with open sodium channels. A naturally occurring indolealkylamine alkaloid, yohimbine, was found to reduce the batrachotoxin-induced Na^+ uptake. The rate of yohimbine inhibition and the rate of its reversal is quite rapid ($\tau_{\frac{1}{2}} \leq 1$ min.). In media containing saturated batrachotoxin (> 1 μM), the dose-response curve of yohimbine can be fitted well by modified Michaelis-Menton relationship with apparent dissociation constant Ka = 1.33 (± 0.17) X 10^{-4} M. Depolarization of membrane potential up to 40 mV does not affect this Ka for yohimbine significantly. By varying the concentration of batrachotoxin, we found that yohimbine is a competitive inhibitor of batrachotoxin. Possible mechanisms for yohimbine to block sodium channel are occlusion of the channel, conformational changes of a specific transporting site in the channel, or interaction with a regulatory or gating molecule to keep the gates closed. The competitive inhibition with a channel opener, batrachotoxin, strongly suggests that yohimbine blocks the sodium channel by acting on the regulatory component or the gating molecules in the membrane.

F-AM-B11 TIME AND TEMPERATURE DEPENDENCE OF RIGHT ANGLE LIGHT SCATTERING FROM LOBSTER SINGLE AXONS DURING EXCITATION. Howard J. Bryant, William S. Bickel, Raphel Gruener, and Rein Kilkson, Marine Biomedical Institute, Galveston, Texas 77550 and Departments of Physics and Physiology, The University of Arizona, Tucson, Arizona 85724.

The differential decay between the right angle light scattering signal and the action potential over a period of several hours was used to study the relationship between the process of excitation and the light scattering signal in lobster single axon. When light scattering was measured at 10°C the scattering signal was usually positive (>95% of axons studied) with respect to the resting scattering level. The scattering as a function of time remained positive and closely paralleled the time course but not the amplitude of the action potential. When the initial scattering was measured at 5°C approximately 50% of the scattering signals were negative with respect to the resting scattering level. With time the negative signals inverted while the action potential amplitude remained essentially constant. When the temperature was elevated to 10°C the negative signal also inverted. The change in sign of the scattering signal was reversable for several temperature cycles after which the signal remained positive, independent of the temperature, until the axon was no longer excitable. We interpret the scattering signal during excitation to reflect changes in membrane index of refraction about a resting level. Depending on initial conditions the resting index may be different. Therefore, the scattering signal during excitation may be positive or negative depending on the initial value of the index of refraction. The index of refraction apparently undergoes a slow change as a function of time which causes an irreversable change in the sign of the scattering signal. This research was supported by an NIH Grant to RG, an NSF Institutional Grant to the University of Arizona and a NIH Post Doctoral Fellowship to HJB.

F-AM-B12 "THRESHOLD" PHENOMENA AND SODIUM SITES AT THE INNERVATED FACE OF THE VOLTAGE-CLAMPED EEL ELECTRO-PLAQUE. T. L. Schwartz, Biological Sciences Group, The University of Connecticut, Storrs, Connecticut 06268.

Large amplitude voltage-clamped depolarization of short duration (50-200 microsec) was followed by a rapid, clamped, return to rest. The membrane responded with a long lasting inward current while held at its resting potential. This current is abolished by TTX and forced to zero when one clamps the membrane to a voltage equal to the "spike" height. The current is thus due to sodium. It is also graded, and saturates as the strength of the triggering depolarization is increased. It peaks before declining, following the briefer depolarizations. After saturation occurs, currents are superimposable when the triggering depolarization lasts between 50 and 500 microsec. When triggering depolarization lasts longer than 500 microsec the current is too large to superimpose on those obtained with briefer triggers. The current displays a "threshold of first appearance" according to the relationship: $\tau(V_t - V_0) = k$, where τ is duration of depolarization, V_t is threshold voltage, and V_0 and k are constants. It is suggested that single sodium sites with a distribution of life-times are synchronously activated by the briefest depolarizations. Depolarizations of sufficient duration can reactivate already relaxed sites, thereby producing increased currents. "Threshold" characteristics under *voltage clamp imply the existence* of a work-function for this phenomenon, as well as a potential range in which site activation is sensitive to small voltage changes.

Supported by Public Health Service Grant NS 08444 and the University of Connecticut Research Foundation.

F-AM-B13 TEMPERATURE DEPENDENT CONDUCTION FAILURE AT AXONAL BRANCH POINTS. R. W. Joyner*, M. Westerfield*, (Intr. by Fidel Ramón), Department of Physiology, Duke University, Durham, N. C. 27710

We have studied the propagation of action potentials through branching regions of squid axons with experimental observations and computer simulations of branching axons over a temperature range of 5°C to 25°C. Theoretical and experimental results show that there is a critical ratio of postbranch to prebranch diameters above which propagation of an action potential will fail. Moreover, this critical ratio is a strong function of temperature, with good quantitative agreement between theoretical predictions and experimental results. The experimentally measured Q_{10} of the critical ratio is -2.7 ± 0.3. Evaluation of a number of parameters of action potential propagation showed that this effect is closely related to the change in the width of the action potential with temperature (Q_{10} = -3.4 ± 0.1).

F-AM-B14 THE EFFECTS OF INJECTED CURRENTS ON COCKROACH MOTORNEURONS, D.J. Meyer and B. Walcott, Dept. of Anatomical Sciences, SUNY at Stony Brook, Stony Brook, N. Y. 11794

In order to systematically investigate the physiological properties of motorneurons in the cockroach Periplaneta americana, we made intracellular recordings from cells in desheathed metathoracic ganglia in situ. The preparation was perfused with physiological saline (Satelle et al. J. Exp. Biol. 62, 1976) containing 5 mM calcium. We identified motorneurons by correlating responses from leg muscles, recorded with electromyographic electrodes, with action potentials recorded from the impaled cell. Initial segment or A spikes never appeared on the leading edge of the motorneuron action potentials, suggesting that there is only one spike initiating zone in these cells. Injection of anodal current pulses (200 ms) elicited trains of action potentials from motorneurons. The relationship between the mean firing frequency during a pulse and the amplitude of the pulse (0.5-20 x 10^{-9} A) was initially linear. Stronger currents elicited progressively smaller increments in firing frequency, resulting in a rolloff in the current frequency relationship. The sensitivity of motorneurons to injected current was related to their actions at the periphery. Motorneurons which produced twitch contractions of muscle (fast motorneurons) had higher thresholds than motorneurons that produced graded contractions. The slope of the current frequency relationship differed for fast and slow motorneurons to the same muscle. We studied the effects of continuous changes of membrane potential on the firing frequency of motorneurons by injecting low frequency (0.5-25 Hz) sinusoidal currents into motorneuron integrating segments. The firing frequency at the peak of the injected waveform was dependent on the amplitude of the current signal but not on its frequency. We also showed that the threshold of fast and slow motorneurons was not dependent on the frequency of the stimulus waveform. Supported by NIH Grant AM 18750.

F-AM-B15 ANALYSIS OF TWO VOLTAGE-DEPENDENT OUTWARD CURRENTS IN APLYSIA INK MOTOR CELLS J. Byrne,* (Intr. by J.N. Howell) Department of Physiology, University of Pittsburgh School of Medicine, Pittsburgh, PA 15261

The release of ink in response to a noxious stimulus is a relatively all-or-none behavior elicited by strong and long lasting stimuli to the animal. It is mediated by three electrically coupled neurons, $L14_{A,B,C}$ in the abdominal ganglion of Aplysia californica (Carew and Kandel Science 192: 150, 1976, and in press). At least some of the features of the behavior are related to a fast transient outward current in the L14 motorneurons (Byrne, Dieringer, Koester and Shapiro, Neuroscience Abstracts 2: 316, 1976). Using voltage clamp techniques the fast transient current and an additional partially decaying delayed outward current were examined. The kinetics of the fast transient current are relatively voltage independent while the rates of activation and decay of the delayed outward current show a marked voltage dependency, increasing with increasing depolarizations. Double pulse experiments revealed that the equilibrium potentials for the two currents are similar and approximately equal to the resting potential of -70 mV. The two currents appear to be carried by potassium ions. Both are blocked by TEA and 4-aminopyridine (4-AP), but TEA is more selective for the delayed current while 4-AP is more selective for the fast transient current. In addition elevated extracellular K^+ reduces both the fast and delayed currents produced by step depolarizations from a fixed holding potential. Using conditioning prepulses to examine the steady state inactivation it was found that the fast transient current is inactivated at levels of about -10 mV, while the inactivation is removed at the resting potential. In addition to these two K^+ currents at least 3 other currents (Shapiro and Koester, this volume), have been identified which also contribute to the firing pattern of the L14 ink motorneurons.

F-AM-B16 IONIC CONDUCTANCES IN INK MOTOR CELLS IN APLYSIA. E. Shapiro* and J. Koester* (Intr. by B. Hoffman). Physiology Dept., Columbia University, N.Y., N.Y.

Voltage clamp studies have revealed 2 voltage-sensitive K^+ conductance channels in the L14 ink motor neurons of Aplysia californica (Byrne, this volume). These cells also have 2 types of conductance pathways for inward current. A TTX-sensitive inward Na^+ current is rapidly activated and inactivated by depolarizations above a membrane potential of -40 mV. Blocking this current by Na^+ removal or TTX reveals a second kind of inward current. In the presence of TTX, action potentials can be elicited by depolarizing pulses only if TEA is also present. The inward current responsible for these TTX-resistant spikes is blocked by 30 mM Co^{++}. This current, which is thought to be carried by Ca^{++}, has threshold and reversal levels about 10 to 20 mV more positive than those of the Na^+ current. The kinetics of activation and inactivation of the Ca^{++} current are slower at all values of membrane potential than those of the Na^+ current. Blocking this inward Ca^{++} current with Co^{++} does not affect the amplitude of delayed rectification or of the fast K^+ current. In addition, prolonged depolarizing pulses (3-10 sec) produce a slow, relatively small build up of outward current, even when delayed rectification and the fast K^+ conductance have been blocked by TEA and 4-AP. Preliminary experiments suggest that this current may flow through a third voltage-sensitive, non-inactivating K^+ conductance channel with very slow kinetics. This slow current could contribute to the spike frequency adaptation which is observed in these cells during long depolarizing pulses. With a more complete description of the currents described in these two abstracts it may be possible to specify fully the ionic mechanisms that determine the role of the L14 cells in inking behavior.

F-AM-C1 ION TRANSPORT ACROSS LIPID BILAYERS MEDIATED BY PROLINE-VALINOMYCIN (PV). O.S. Andersen*, A.A. Lev*, M. Fuchs*, P. Ting-Beall*, and D.C. Tosteson, Dept. Physiol., Cornell Univ. Med. Coll., New York and Dept. Physiol. and Pharmacol., Duke Univ. Sch. Med., Durham, N.C. (intro. by E.E. Windhager).

Membrane conductance behavior of glycerolmonooleate bilayers doped with PV was investigated using a voltage-clamp technique. When the aqueous phases contain K^+, Rb^+, Cs^+, NH_4^+ or Tl^+ one observes current transients which are exponential for more than 4 time constants, and which continue with a time course consistent with aqueous diffusion polarization. Charge movement during the initial transient is therefore essentially confined to the membrane interior. Charge movement was studied as a function of applied potential. The transferred charge reaches an upper limit with increasing potential. A further analysis of charge transfer as a function of potential indicates that the movement of PV-ion complexes are influenced by only a fraction (0.8 - 0.9) of the applied potential. In 1 M salt the initial conductance and charge absorption are linear functions of the aqueous PV concentration up to about 10^{-6}M. The absorption coefficient for PV-K^+ is 0.004 cm. The time constant for transfer of PV-ion complexes across decane-containing membranes is 0.58 msec for K^+, 0.33 msec for Rb^+, and 0.76 for Cs^+. The aqueous dissociation constant (K_D) between PV and K^+, Rb^+, and Cs^+ were determined by studying the dependence of charge absorption, or initial conductance, on the aqueous concentration of these ions. Ionic strength was held constant at 1.0 M with NaCl. K_D for K^+ is about 40 mM, while K_D for Rb^+ and Cs^+ both are about 20 mM.

Partially supported by NIH grants, HL12157 and GM21342. Olaf S. Andersen is a New York Heart Association Senior Investigator.

F-AM-C2 MECHANISM OF ION TRANSPORT MEDIATED BY PV-LAC IN LIPID BILAYER MEMBRANES. Walter J. Koroshetz*, Ramon Latorre, Balz F. Gisin and Daniel C. Tosteson, Department of Pharmacological and Physiological Sciences, University of Chicago, Chicago, Ill. 60637

PV-Lac is an analog of valinomycin with the following primary structure: cyclo-(L-val-D-pro-D-val-L-lac)$_3$. From steady state conductance measurements we have found that the selectivity sequence, relative to K^+, for PV-Lac in phosphatidyl ethanolamine (PE) membranes is: Cs, 0.5; NH_4, 0.28; Na, 0.1; Li, 0.01. This sequence is similar to the one obtained with valinomycin and peptide PV but the ratio of the steady state conductance in Na^+ to that in K^+ is 0.1 with PV-Lac as compared to 10^{-3} for valinomycin. In all experiments with K^+, NH_4^+ and Cs^+ the steady state current reaches a maximum with potential. However, in all experiments with Na^+ and Li^+ current increases in a superlinear fashion with potential. We have also investigated the kinetics of ion transport mediated by PV-Lac. To do so we analyzed the relaxation of membrane current after a voltage jump. From the relaxation data the translocation rates for the PV-Lac -K^+ complex and absorption coefficients between membrane and water have been calculated. In PE membrane the rate constant for translocation (k_{ms}) is 41 sec^{-1} and the absorption coefficient is 2.75×10^{-4} cm. In monoolein membranes the k_{ms} for the K^+-complex is 2×10^4 sec^{-1} and the absorption coefficient is 1.35×10^{-3} cm. Furthermore, analysis of the current relaxation experiments indicate that PV-Lac complexes with K^+ in the aqueous solution and not at the membrane-solution interface as in the case of valinomycin.

(Supported by Grant NIH-HL-19951-01)

F-AM-C3 TRI-BUTYL TIN PRODUCES CHLORIDE EXCHANGE DIFFUSION IN BILAYERS. M.T. Tosteson, J.O.Wieth and D.C. Tosteson, University of Chicago and University of Copenhagen.

Tri-butyl tin (TBT) has been reported to produce chloride-hydroxyl exchange in inner mitochondrial and red cell membranes (Selwyn et al., Euro J. Biochem.14:120,1970). One of us (J.O.W.), has described TBT-induced chloride exchange diffusion in human red cell membranes. This report describes experiments which show that TBT produces chloride exchange diffusion in planar bilayers made from phosphatidyl ethanolamine dissolved in n-decane. Bilayers were formed in a solution of KCl (0.1M) and K_2HPO_4-KH_2PO_4 (0.001M, pH 7.4). A tracer amount of $^{36}Cl^-$ was added to one bathing solution and Cl^- flux estimated from the rate of appearance of $^{36}Cl^-$ on the opposite side of the membrane. Steady state membrane electrical conductance was measured simultaneously. In the absence of TBT, Cl^- flux was too low to measure by our technique ($< 10^{-12}$moles $cm^{-2}sec^{-1}$) and membrane conductance was about 10^{-8} $ohm^{-1}cm^{-2}$. When TBT (6×10^{-6}M) was present in one bathing solution, Cl^- flux was 1.7×10^{-9}moles $cm^{-2}sec^{-1}$and membrane conductance increased to about $5 \times 10^{-8}ohm^{-1}cm^{-2}$. Cl^- flux was not influenced by imposed changes in the electrical potential difference across the membrane. Furthermore, Cl^- conductance calculated from the assumption that all of the Cl^- flux can carry charge was $2 \times 10^{-1}ohm^{-1}cm^{-2}$, far in excess of the measured total electrical conductance of the membrane under these conditions. Therefore, in the presence of TBT, Cl^- crossed the membrane primarily by a mechanism that cannot transfer charge. Since the maximum rate at which TBT could diffuse across the unstirred layers of aqueous solution bathing the membrane surface in this experiment was 6×10^{-12}moles $cm^{-2}sec^{-1}$, it is apparent that Cl^- transport occurs by exchange diffusion rather than diffusion of TBT.Cl ion pairs.

Supported By NIH Grant HL-19951-01.

F-AM-C4 ELECTRICALLY SILENT TRANSPORT OF INORGANIC ANIONS ACROSS LIPID BILAYER MEMBRANES. John Gutknecht, Department of Physiology and Pharmacology, Duke University, and Duke University Marine Laboratory, Beaufort, N.C. 28516.

Electrically silent anion transport occurs in many plant and animal cell membranes. The transport process may be either an anion exchange (e.g., Cl^--Cl^- or Cl^--HCO_3^-) or a cotransport of a cation and an anion (e.g., Na^+ and Cl^-). In order to gain insights about the mechanisms of anion transport, we are studying the effects of various lipids and proteins on Br^- fluxes across planar lipid bilayers. Br^- fluxes are measured with $^{82}Br^-$ (in NaBr), and $S_2O_3^=$ (1 mM) is added to prevent the formation of $^{82}Br_2$. The electrically silent anion flux is estimated by comparing the one-way flux with the flux predicted from the membrane conductance. We have found high rates of electrically silent Br^- transport in several types of membranes. For example, membranes made from equimolar amounts of a secondary amine (n-lauryl[trialkylmethyl]amine) and egg lecithin in decane showed anion fluxes comparable to those in erythrocytes ($\geq 10^{-8}$ mol/cm^{2}sec). The secondary amine behaves as a "titratable carrier" for Br^-, the flux being roughly proportional to the H^+ concentration over the pH range of 5.5 to 7.5. At pH <5 the flux becomes rate limited by diffusion of Br^- through the unstirred layers, and at pH >8 the Br^- flux becomes constant at about 10^{-10} mol/cm^{2}sec, which is probably due to a cotransport of Na^+ and Br^-. We have also observed electrically silent Br^- transport with bovine carbonic anhydrase (CA) in the aqueous solutions. The membrane in this case was decane and bovine phosphatidylserine which we used by mistake, thinking it was egg lecithin. In the presence of CA (1 mg/ml) the Br^- fluxes were 100-200 pmol/cm^{2}sec, whereas the control fluxes were 10-20 pmol/cm^{2}sec. These results, although preliminary, support several other reports that CA may function as an anion carrier in plant and animal cell membranes. (Supported in part by USPHS Grant HL 12157.)

F-AM-C5 Na^+ SELECTIVE PERMEATION OF LIPID BILAYERS MEDIATED BY A NEUTRAL IONOPHORE. K.-H. Kuo and G. Eisenman, Dept. of Physiol., U.C.L.A., Med. Sch., Los Angeles, Ca. 90024.

Na^+ selective permeation across lipid bilayers has heretofore not been successfully accomplished in vitro despite the existence of a variety of lipophilic Na^+ complexing molecules (e.g. antamanide). We here report the first example of an artificial lipid bilayer system which is selectively permeable to Na^+. This was achieved using the Na^+ selective molecule (see figure) synthesized and characterized in bulk electrodes by Ammann, Pretsch, and Simon (Anal. Lett., 7 (1974), 23) which we find renders GMO bilayers selectively permeable to Na^+ as judged by potential and conductance. The conductance is proportional to the 1st and 2nd powers of cation and ionophore concentration, respectively (.0003 ohm^{-1} cm^{-2} at 1.0M NaCl and 2x10^{-5}M ionophore); and the I-V characteristic is "hyperbolic". Like nonactin but unlike gramicidin, the conductance is 10^3 greater in GMO then PE bilayers (and is 10^3 higher in black than in colored films). A Nernst response is seen for Na^+ and the membrane potential is described by the GHK equation in ionic mixtures, with anion permeabilities which can exceed those for some cations. The permeability ratios among cations (and anions) as defined by the GHK equation in GMO/decane (fig.) are concentration- and voltage-independent, but the ratio between cations and anions depends on concentration. Permeability ratios also agree with conductance ratios and with selectivity seen by Simon et al. for bulk electrodes, which suggests a carrier mechanism. (Supp. by (NSF GB 30835 and USPHS NS 09931))

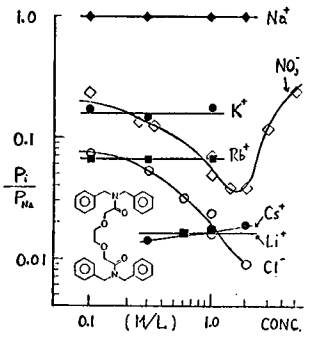

F-AM-C6 MECHANISM OF ELECTRICAL CONDUCTIVITY OF LECITHIN-CHOLESTEROL BILAYERS INDUCED BY 2,4-DICHLOROPHENOXYACETIC ACID. P. Smejtek, and M. Paulis† Department of Physics, Environmental Science Program, Portland State University, Portland, Oregon 97207

Past studies of action of weak acid uncouplers of oxidative phosphorylation on lipid membranes have revealed that the increase of membrane electrical conductivity observed in their presence is due to the permeation of either the conjugated anion of the acid or due to a negatively charged dimer complex formed by the association of one neutral and one ionized acid molecule. We have studied steady-state electrical conductivity induced by 2,4-Dichlorophenoxyacetic acid (2,4-D) and observed that (a) the conductivity is independent of pH at pH<pK (2.7) and decreases with pH at pH>pK, (b) the conductivity increases quadratically with 2,4-D concentration, and (c) the conductivity is proportional to concentration of alkali ions. The experimental results are compatible with the hypothesis that the current carrying species in the membrane is a positively charged complex formed by the recombination of two neutral molecules of 2,4-D with one monovalent cation. We have also observed an increase of the rate of transport of Nonactin-K^+ complex across the membrane in the presence of the neutral form of 2,4-D. Experiments have been designed to determine whether this effect is due to the lower height of the membrane permeability barrier with respect to cations or due to the increase of the density of K^+ ions at the membrane surface *in the presence of* 2,4-D.

This work is supported by NIH grant R01 ES937.

F-AM-C7 ELECTRICAL CONDUCTIVITY OF LIPID-CHOLESTEROL MEMBRANES INDUCED BY PENTACHLOROBENZENETHIOL. K. Hsu, P. Smejtek, R. Jayaweera‡ and A. Valdez‡ Department of Physics, Environmental Science Program, Portland State University, Portland, Oregon 97207

Pentachlorobenzenethiol (PCBT), an analogue of pentachlorophenol (PCP), is an uncoupler of oxidative phosphorylation. Wilson, Ting, and Koppelman† have studied the uncoupling activity of PCBT in rat liver mitochondria and concluded that pH dependence of PCBT uncoupling activity and that of electrical conductivity of lipid bilayer membranes are unrelated. We have studied the PCBT induced electrical conductivity in lecithin-cholesterol-decane membranes under various conditions. We found that when PCBT is in the aqueous medium the membrane conductivity increases slowly with time and does not reach a stationary level within the life-time of the membranes (several hours). This steady increase of conductivity can be explained by the high partition coefficient of PCBT between the membrane phase and the aqueous phase, and the redistribution of PCBT between the membrane torus and the bilayer. Meaningful conductivity data can be obtained only when PCBT is incorporated into the membrane forming solution. PCBT in solutions was found to be light sensitive, and dimerizes readily at room temperature. The dimers are electrically inactive. Careful measurements of the pH dependence of PCBT induced membrane conductivity have revealed a well developed bell-shaped curve similar to that found for PCP, but with the position of the maximum shifted by about 2 pH units above the pK value. This pH profile agrees rather well with that for PCBT observed by Wilson et al. In contrast to PCP, the PCBT induced membrane conductivity decreases with voltage, which indicates the presence of severe kinetic limitations in the charge transfer process across the membrane. [This work is supported by NIH grant RO ES937.]

†Biochemistry, 10:2897, 1971.

F-AM-C8 ALAMETHICIN INDUCED FLUCTUATIONS IN LIPID BILAYERS. W. O. Romine & R. J. Bradley, The Neurosciences Program, University of Alabama Medical Center, Birmingham, AL 35294

Alamethicin induced fluctuations of conductance in bilayers have been analyzed using stationary time series analysis. Measurements were made between +60 and -60 mV, encompassing the negative resistance region. At positive potentials, the power spectrum revealed two time constants. The slower time constant was significantly voltage dependent, varying from 0.35 sec (+60 mV) to 0.11 sec (+10 mV), and is probably associated with cluster formation as reported by Haydon and coworkers. The faster time constant (27 ms) exhibits negligible voltage dependence and is likely associated with transitions between preferred conductance states within a cluster. At negative potentials, the power spectrum shows three rather than two time constants, becoming apparent at the beginning of the negative resistance region. The slow time constant is still probably associated with cluster formation and shows very marked voltage dependence, changing from a minimum of 0.11 sec at +10 mV to 2.7 sec at -60 mV. The medium speed time constant (40 ms) shows no detectable field dependence and is likely associated with transitions between preferred conductance states. The high speed time constant observed is marginally voltage dependent, changing from 4.0 ms to 5.3 ms (-25 to -60 mV). Haydon and coworkers have shown that at positive potentials, the preferred conductance levels within a cluster are the lower levels, whereas at negative potentials, the higher levels are preferred. Thus, at negative potentials, the third time constant might be associated with the rapid transition from the initial cluster formation to the higher states. The marked increase in the cluster formation time constant between -15 and -30 mV probably accounts for the decrease in membrane conductance and the associated negative resistance region.

Supported by NSF Grant #BNS 7514321 and an NSF Predoctoral Fellowship to W.O.R.

F-AM-C9 INTERPRETATION OF ALAMETHICIN-INDUCED ION CONDUCTANCE IN LIPID MEMBRANES. C. Eldridge* and H. J. Morowitz, Yale University, New Haven, Ct. 06520

A mechanism for discrete conductance fluctuations in alamethicin-modified black lipid membranes [Gordon and Haydon, BBA 225:1014(1972); Eisenberg et al., J. Memb. Biol. 14:143 (1973)] is proposed. We suggest that a pore is a modular structure with several similar ion channels, each of which may open and close independently, but all activated simultaneously. This model contrasts sharply an earlier proposal that the alamethicin pore undergoes discrete enlargements [Baumann and Mueller, J. Supr. Struct. 2:538(1974); Boheim, J. Memb. Biol. 19:277(1974)]. Two lines of evidence back this model. First the histograms of conductances consistently may be described by a binomial distribution function. At room temperature the probability of a single channel being open is around 0.5, giving very characteristic conductance distributions corresponding to rows of Pascal's triangle. At 33°C the distributions become skewed corresponding to $P_{(open)} = 0.4$. This result also leads to calculation of ΔH and ΔS for the open-closed transition. The second line of evidence is the observation of nearly regular conductance spacings under a variety of conditions. The deviations of these spacings from regularity were the basis of the expanding pore model, but the expanding pore model has two distinct drawbacks: (1) It contradicts observations by Gordon and Haydon [Phil. Trans. Roy. Soc. Lond. B270:433(1975)] that spacings at all levels decrease when large cations are used. (2) It predicts larger-than-observed variance in conductance spacings when a hydrodynamic conductance theory [Levitt, Biophys. J. 15:533(1975)] is used to predict conductances from hypothetical pore and cation radii. We present data showing that conductance spacings are regular, within observation error, with several different cations and lipids. Local alterations of Born charging energies may be responsible for the deviations from uniform conductance spacings.

F-AM-C10 ION TRANSPORT THROUGH THE HEMOCYANIN CHANNEL. Osvaldo Alvarez*, Juan Reyes* and Ramon Latorre, Department of Pharmacological and Physiological Sciences, University of Chicago, Chicago, Ill. 60637, and Faculty of Sciences, University of Chile.

When hemocyanin is added to a black lipid film the conductance increases in discrete steps which represent the formation of channels across the membrane. Comparison of the conductance steps, for different salts, allows us to obtain an ion selectivity sequence. These results can be compared with those obtained from standard bi-ionic potential measurements. Our results obtained by measuring bi-ionic potentials indicate that the hemocyanin channel is ideally selective to cations (it excludes anions). The permeability ratios for alkali metals, relative to K^+ are: Cs^+, 0.98; Rb^+, 1.0; K^+, 1.0; Na^+, 0.79 and Li^+, 0.32. Our measurements indicate that the single channel conductance shows saturation properties for all alkali metal tested. The single channel conductance is well described by an hyperbolic function of salt concentration in the range from 20 to 500 mM. Conductance ratios measured at 100 mM relative to K^+ are: Rb^+, 0.98; K^+, 1.0; Na^+, 0.75 and Li^+, 0.19. The selectivity sequence obtained by bi-ionic potential measurements and single channel conductance are in agreement. The relative permeabilities are proportional to the ionic mobilities in free solution with the exception of Li^+. Comparison of single channel conductances for the different monovalent cations shows that there is an abrupt cut-off in the permeability to Li^+.

(Supported by Grants NIH-HL-19951-01 and the University of Chile)

F-AM-C11 CYANINE DYE-INDUCED ELECTRICAL AND FLUORESCENCE EFFECTS IN NEUTRAL AND NEGATIVE BILAYER MEMBRANES. S. Krasne, Dept. of Physiology, UCLA Med. Sch., Los Angeles, Calif. 90024

Electrical measurements were made on planar bilayer membranes, containing phosphatidyl ethanolamine (PE), in the presence of the cyanine dyes $diSC_n(5)$, where n=1,2,or 3. These dyes increase the membrane permeability ideally for anions. The membrane conductance increases with the 4th or 5th power of the dye concentration, and the conductance is lower if the membrane also contains phosphatidyl serine (PS). The dyes also increase membrane surface potentials, this effect being greater for longer chain length dyes and for more negatively-charged membranes. The change in surface potential is $\lesssim$+58mV for dye concentrations $\lesssim 10^{-5}$M and ionic strengths of 10^{-1}M. Dye-induced conductance changes in PE membranes increase steeply with increasing transmembrane potentials. The steepness of the conductance-voltage relationship increases with increasing dye concentration, and rectification is observed when the dye concentrations either side of the membrane are unequal. In PE/PS (1:1) membranes, the conductance saturates with increasing voltage at lower dye concentrations and is independent of voltage at higher dye concentrations. The potential dependence of $diSC_2(5)$ fluorescence in liposomes composed of phosphatidyl choline (PC) or PC/PS (4:1) mixtures parallels the observations on membrane conductance and surface potentials. Namely, more dye adsorbs to negatively-charged, PC/PS, than to neutral, PC, liposomes, and the fluorescence-voltage relationship is much steeper in neutral than in negatively-charged liposomes. These cyanine-induced electrical and fluorescence effects can be rationalized by a model which assumes that, within the membrane, dyes form aggregates which 1) are anion-selective channels, 2) increase with increasing (negative) potential or dye concentration, 3) do not cross the membrane, and 4) are adsorbed to a saturable number of membrane sites.

F-AM-C12 PHOTOELECTRIC EFFECTS IN DYE-SENSITIZED ARTIFICIAL LIPID MEMBRANES. James M. Mountz* and H. Ti Tien, Biophysics Department, Michigan State University, East Lansing, Michigan 48824

Photovoltage generation by artificial lipid membranes in the presence of a series of dyes with known redox potentials have been observed. A systematic series of experiments has been performed in which the dark and photo-induced voltages were measured for each of these compounds. Using electronically conducting membranes, the standard redox potentials are correlated with the open circuit voltage measurements. The object of this investigation was to show how these dyes behaved as light sensitizers for bilayer lipid membranes (both modified and unmodified) that contained no other photoactive compounds.

F-AM-C13 PHYCOCYANIN ENHANCEMENT OF BLM PHOTORESPONSE. S. M. Adams and S. Chen*, Division of Laboratories and Research, New York State Department of Health, Empire State Plaza, Albany, NY 12201

Bilayer membranes (BLM) of the Rudin-Mueller type were analyzed for their photoresponse in the presence and absence of Cyanophyte phycocyanin. When bilayer membranes were formed from a chloroplast extract solution derived from spinach leaves, the photoresponse in pH 5 buffer was of the order of several millivolts. Modification of the electrochemical gradient across the membrane directly affected the magnitude and polarity of the photoresponse. When phycocyanin from Plectoneme calothricoides was added to the oxidized side of the membrane, a two-fold enhancement of the photoresponse was observed. A completely synthetic membrane-forming solution, composed of 4 mg/ml dioleoyl phosphatidyl choline (lecithin), 2 mg/ml chlorophyll a, and 1 mg/ml β-carotene, gave similar photoresponses as the membrane obtained from chloroplast extract solutions. The membrane resistance and capacitance were similar to those values obtained from chloroplast extract BLM. However, addition of phycocyanin to the oxidized side of the membrane did not result in the usual enhancement of the photoresponse. A similar membrane-forming solution using natural egg lecithin also gave a BLM whose photoresponse was unaffected by phycocyanin. Apparently, not all photosensitive chlorophyll-containing phospholipid BLMs are responsive to phycocyanin-stimulated enhancement. It is possible that a specific lipid constituent is required or a complex mixture of lipids is needed for the phycocyanin to be effective.

This work was supported in part by Grant 1R01 GM22247-01 from the National Institutes of Health.

F-AM-C14 LOCATING CYANINE DYES IN BILAYER MEMBRANES THROUGH THEIR PHOTO-VOLTAGE WAVEFORMS. Jay S. Huebner, Dept. of Natural Sciences, Univ. of North Florida, Jacksonville, FL 32216

The positions the illustrated dye molecules occupy in bilayer membranes is deduced from voltage waveforms which follow flash illumination. The results indicate these dyes are amphipathic; oxygen atoms and electric charge produce hydrophilic forces, while alkyl groups produce lipophilic forces. Optical excitation apparently partially confines the dye's delocalized charge, making the dye temporarily more hydrophilic. The n=1 dye is impermeable & occupies one membrane surface (when added to the positive electrode solution only). It induces a positive monophasic waveform following illumination, as adsorbed dye moves toward the adjacent aqueous solution[1]. Positive transmembrane voltages, imposed from a high impedance source, reposition the adsorbed dye further into the membrane. This decreases the dielectric force resulting from charge localization, which decreases the waveform risetime and increases its amplitude. Negative voltages have the opposite effects. The n=2 & 3 dyes are semi-permeable and occupy both membrane surfaces. Imposed voltages induce biphasic waveforms which are similar to waveforms obtained at the same voltage when n=1 dye is added to both sides of the membrane. Dyes with n=4 to 18 are permeable and induce monophasic photovoltages with imposed voltages as excitation temporarily lowers the dyes' permeability, temporarily increasing the membrane resistance. The increased lipophilic force for n=4 & 6 results in these dyes being absorbed primarily in the membrane core. For $n \gtrsim 8$ the waveform amplitude varies with light polarization, indicating these dyes absorb so their optical absorption moment is parallel to the membrane. Apparently the $n \gtrsim 8$ molecules extend from the core into the surface layer where the chromophoric groups are ordered. Support by NIH (GM 23250) and the gift of dyes from A. Waggoner are acknowledged.

[1] J. S. Huebner, Biochim. Biophys. Acta 406 (1975) 178-186.

F-AM-C15 MECHANISM OF MEMBRANE POTENTIAL SENSITIVITY OF MEROCYANINE 540. P. R. Dragsten* and W. W. Webb (Intr. by R. M. Spanswick), Physics Department and School of Applied and Engineering Physics, Cornell University, Ithaca, N.Y. 14853

Fluorescence polarization measurements performed on hemispherical lipid bilayer membranes stained with merocyanine 540 have revealed the probable mechanism of its membrane potential sensitivity. The dye was introduced into one side of the membrane and transient fluorescence changes monitored while voltage pulses were applied across the membrane. Transient response on two time scales, fast ($<10^{-5}$ sec) and slow ($\sim 10^{-1}$ sec), was observed. The slow response is apparently due to a membrane chromophore concentration change with kinetics determined by diffusion across the unstirred boundary layer ($\tau \sim k_a^2/D$) [Conti et al., Biophys. Struct. Mech. 1, 27 (1974)]. The partition coefficient k_a and the chromophore diffusion coefficient D in the solution were determined by fluorescence correlation spectroscopy [Magde et al., Biopolymers 13, 29 (1974)]. The fast response appears to be due to reorientation of the chromophore molecule in the applied electric field. A negative voltage pulse applied to the labeled side of the membrane stimulated a transient decrease of the fluorescence excited in chromophore molecules oriented parallel to the membrane and a transient increase of the fluorescence excited in molecules oriented perpendicular to the membrane. Reduction of the fluorescence signal from the parallel orientation at high chromophore concentrations suggests effects of formation of non-fluorescent dimers in the parallel orientation [Tasaki et al., Biophys. Chem. 4, 1 (1976)]. A simple kinetic model has been developed that accounts for the observations quantitatively. The hypothesized fast molecular reorientation mechanism is consistent with the molecule's structure, probable electric dipole moment, and reported fluorescence and absorption signals in axons.

F-AM-D1 WET CHROMATIN STRUCTURE. S. Basu and D. F. Parsons, New York State Department of Health, Division of Laboratories and Research, Albany, NY 12201.

The wet replication technique[1] using a differentially pumped hydration chamber in a high vacuum evaporator has been applied to chromatins. Fresh rat liver nuclei were surface spread in the presence of 1-2 mM EDTA and then immediately (1 mm) picked up on hydrophilic grids containing replication markers of fixed diameter. The chromatins were replicated by SiO at equilibrium water vapor pressure or slightly above (26 TORR, 25°). The chromatins released from osmotically shocked nuclei represent fibers which have considerable degree of thickness variation along their length, namely, from about 50 nm to 8 nm. Chromatins which are completely released from the disrupted nuclei are kinky or wavy resembling the surface of a slow turning helix. These fibers also terminate into a 80 Å fiber. In some occasion the 50 nm fiber has shown thickness jump over discrete lengths e.g., from 50 nm to 8 nm, 8 nm to 50 nm and then from 50 nm to 25 nm etc., while the chromatin is still continuous being embedded in the water layer. The chromatin structure seems to be affected by partial drying and by the presence of excess (e.g., 2 mM) EDTA and these effects are being studied. (Supported by USPH Grant GM-16454. Thanks are due to Dr. S. Bram and J. LePault who kindly prepared the nuclei for us.)

[1] S. Basu and D. F. Parsons (1976) J. Appl. Phys. 47, 741,752.

F-AM-D2 WET CHROMOSOME STRUCTURE. S. Basu and D. F. Parsons, New York State Department of Health, Division of Laboratories and Research, Albany, NY 12201.

The wet replication technique[1,2] using a differentially pumped aperture limited hydration chamber in a vacuum evaporator has been applied to study the wet surface features of Chinese hamster chromosomes. Hypotonic cells at neutral pH containing dislodged intracellular chromosomes are surface spread by a gentle method[3]. Hydrophilic grids are touched on the spread material because such substrate allows attachment of chromosomes onto the substrate in large numbers and also because such substrate facilitates flattening of the water layer to an ultrathin level (3 nm). The thinning of water layer is determined by replicating small markers up to 9.1 nm in diameter simultaneous with the wet chromosomes. Wet chromosomes represent intact shape and fibrous morphology which are both lost on vacuum drying or critical point drying. The chromosomes in whole metaphase plates suggest several important pieces of information. The telomere of one chromosome is often attached to a near centromeric region of its next partner. The fibers bridging the successive chromosomes are about 35 nm in width. The free telomeres of some chromosomes show attachment of microtubular fibrils which are highly branched and in some cases are even up to 20 Å in width. The surface of any chromosome is highly knobby (i.e beaded) but very rarely links between them can be seen. The knobs are about 18 nm in diameter. Several fibers (23 nm diam.) are seen longitudinal in the centromeric regions, which then terminate into the telomeres. The contour of these fibers inside the chromosomes i.e., their regular folding pattern is expected to be unfolded in the scanning transmission mode. (Support by USPH Grant GM-16454.)

[1,2] S. Basu and D. F. Parsons (1976) J. Appl. Phys. 47, 741,752.

[3] D. F. Parsons (1965) Methods in Enzymol. 10, 101.

F-AM-D3 SIZES OF DNA HELIX OPENINGS WITHIN INTACT CELLS DURING IN-VIVO GENE REGULATION. J.H. Frenster, S.R. Landrum*, M.L. Masek*, S.L. Nakatsu*, and L.S. Wilson*, Department of Medicine, Stanford University, Stanford, Calif. 94305.

Localized openings of the DNA helix are necessary to allow strand-selective gene transcription at that particular gene locus within living mammalian cells (Cancer Res. 36, 3394 (1976). These DNA helix openings can be visualized within individual living cells by a high-resolution electron microscopic probe technique (Nature New Biol. 236, 175 (1972), and their number and size can be determined within each cell (Nature 248, 334 (1974). 742 normal and neoplastic cells within biopsied human bone marrow and lymph nodes were analyzed for the localization, number, and size of DNA helix openings within each cell, and this data was then separately correlated with the ultrastructure of each cell. All DNA helix openings were confined to the extended euchromatin portion of the cell nucleus. The number of DNA helix openings was increased during cell activation and decreased during cell maturation. The sizes of DNA helix openings ranged from 0.025 microns to 0.7 microns, with the large openings confined to less mature normal and neoplastic cells. This size range of DNA helix openings corresponds to a range of 70-2000 nucleotide base pairs. The size distribution of DNA helix openings was skewed toward larger openings within immature cells and toward smaller openings within mature cells. These quantitative single-cell data suggest that greater numbers of large gene loci are transcribed within active immature cells than are transcribed within less active mature cells. Supported in part by Research Grants CA-10174 and CA-13524 from the National Cancer Institute, IC-45 from the American Cancer Society, and by a Research Scholar Award from the Leukemia Society.

F-AM-D4 PARTIAL PURIFICATION AND TRANSLATION OF mRNA FOR GLUTAMATE DEHYDROGENASE FROM EUKARYOTIC CELL. M.Hillar, V.Lott* Department of Biology, Texas Southern University, Houston, Tx. 77004

Poly(A)-mRNA for glutamate dehydrogenase was purified about 1000 times from rat liver ribosomes. RNA was extracted with the phenol : chloroform procedure and was next fractionated on poly(U)-agarose column and poly(A)-mRNA fraction was obtained.

These RNA fractions were characterized with respect to their secondary structure, poly(A) content and were further fractionated on sucrose density gradient and tested for glutamate dehydrogenase template activity in a cell-free systems with microsomes or polysomes.

Biosynthesise of enzyme was followed spectrophotometrically using dual wavelength technique. Also products of translation were identified using labeled amino acids by density gradient and electrophoresis of immunoprecipitates. Supported by NIH # PR 0806 and T.S.U. # 16-909.

F-AM-D5 A SMALL CELL WITH NOVEL BIOLOGICAL FEATURES. J. Maniloff, A. Ghosh*, and J. Das*, Dept. of Microbiology, University of Rochester, Rochester, N.Y. 14642.

The smallest free living cells, the mycoplasmas, are interesting model cellular systems. We have shown that one particular species, Mycoplasma gallisepticum, has certain unique features. First, these cells have the smallest reported genome size, 4.6×10^8 daltons. The DNA is 35% GC and is replicated one per cell doubling (J. Bact. 115:117, 1973). Second, studies of the cells' rRNA have shown that it has significantly different oligonucleotide sequences than other prokaryotes (Woese and Maniloff, MS in preparation). The cells' ribosomes readily condense into helical superstructures (PNAS 68:43, 1971). Third, although the cells are small (about 0.5 um), each cell has specialized polar subcellular organelles at which DNA replication takes place. It has been proposed that these organelles function as a primitive mitotic-like apparatus, involved in chromosome organization and segregation (J. Bact. 120:495, 1974). Fourth, these cells have neither dark repair nor photoreactivation mechanisms for the repair of UV induced DNA damage. The UV inactivation curve indicates that each cell contains only a single genome copy. Studies of irradiated cells' DNA show that UV induced dimers are not excised and block further replication. Fifth, this is the only prokaryote which can be inhibited by cytochalasin B. Our data suggest that cytochalasin B affects structural components required for cell division. We will review our recent data on items 4 and 5. It is believed that these small cells may have a tight coupling between DNA replication and cell division: the subcellular organelles, functioning by a cytochalasin B sensitive process, may be necessary to assure segregation of the two daughter genomes to opposite ends of the dividing cell. The UV and rRNA results allow us to consider various possibilities for the evolution of these small cells. (Supported by USPHS Grant AI 07939).

F-AM-D6 THE ORGANIZATION OF PRIMATE GENOMES AS ASSESSED BY HIGH RESOLUTION THERMAL DENATURATION. D. L. Vizard and A. T. Ansevin, Department of Physics, M.D. Anderson Hospital and Tumor Institute, Houston, Texas 77030.

High resolution thermal denaturation, when applied to eukaryotic DNAs, demonstrates discrete subpopulations (thermalites) that denature within a small temperature range. We identify these thermalites with highly repeated DNA sequences, and find significant qualitative and quantitative differences among the thermalites of African Green monkey, Rhesus monkey, Human, and HeLa cells. Denaturation profiles of high molecular weight DNAs ($>25 \times 10^6$au) which have been renatured after incomplete denaturation, demonstrate that most of the primate thermalites represent sequences that are physically linked to a small fraction of highly stable DNA. Further, assessments of the renaturation process imply that the sequences immediately adjacent to the stable fraction are randomly distributed with respect to their denaturation temperature. (Supported by NIH Grant GM 23067)

F-AM-D7 IMMUNOLOGICALLY SPECIFIC AND TRANSCRIPTIONALLY ACTIVE FRACTION OF RETICULOCYTE CHROMATIN. K. Hardy*, J.F. Chiu, and L.S. Hnilica*, Department of Biochemistry, Vanderbilt University School of Medicine, Nashville, Tenn. 37232.

Reticulocyte chromatin fixed the complement strongly in the presence of specific antiserum. Under the same conditions, erythrocyte chromatin was inactive. Experimental evidence indicated that the nuclear reticulocyte-specific antigens exist in the form of DNA-nonhistone protein complexes. The possibility that these tissue-specific nuclear antigens may be related to the regulation of transcriptional activity was also investigated. Erythrocyte and reticulocyte chromatins were fractionated into transcriptionally active and inactive fractions by shearing and fractionation with divalent cations (Hardy et al., Fed. Proc. 35, 1960, 1976). The active fraction of reticulocyte chromatin transcribed globin mRNA-like sequences over 100 times more efficiently than the inactive fraction of the same chromatin. The globin mRNA-like transcription by the active fraction of erythrocyte chromatin was very low. The immunologically tissue specific nuclear antigens of reticulocytes were found accumulated in the active fraction of chromatin. The transcriptionally inactive fraction of reticulocyte chromatin was also inactive immunologically. Electrophoretic analysis of chromosomal nonhistone proteins from the active and inactive fractions of the same chromatin showed significant differences in the distribution of 5 or 6 protein bands. Even more prominent differences were observed when nonhistone proteins from erythrocyte and reticulocyte active fractions were compared. Our results indicate that a small fraction of chromosomal nonhistone proteins found to be present only in reticulocytes may be responsible for their immunological specificity as well as for the regulation of globin gene transcription. Supported by NCI grant CA 18389 and The National Foundation March of Dimes Grant No. 1-493.

F-AM-D8 PHYSICAL STUDIES OF MIXED RECONSTITUTED COMPLEXES FROM G_1 AND S PHASE PROTEINS WITH DNA. P. Miller, T. Dolby,* T. Borun,* S. Gilmour* and C. Nicolini. Biophysics Division, Temple University, Philadelphia, Pa. 19140

Dichroism spectroscopy (C.D.) is utilized in order to detect changes prior to helix-coil transition, which reflect subtle changes in the asymmetry of the DNA, as superhelix to helix transition (Miller et al, N.A.R., 3, 1875, 1976). G_1 DNA was found to be only slightly more stable to thermal denaturation than either M or S phase DNA. G_1 native chromatin is quite more stable than S phase native chromatin compatable with higher degree of supercoil in G_1 as suggested also by independent physical-chemical studies (Nicolini et al J.B.C. 250, 338). Reconstituted G_1 and S phase chromatins show frequently a partial recovery of the native superpacking, but the CD-thermal denaturation profiles fails to reproduce the difference among their respective native chromatins. Mixed reconstitutions of cell cycle stage-specific histone and non-histone proteins with high molecular weight DNA, were studied using molar ellipticity as a function of temperature to ascertain the role of cell cycle stage-specific chromosomal proteins on chromatin stability. The data suggest that both histone and non-histone fraction differentially contributes to the observed CD melting profiles. Specifically, the non-histone chromosomal proteins seems to be responsible of the decrease thermal stability during the G1-S transition. (Supported by NIH Grant CA18258 and CA20034).

F-AM-D9 NEWLY SYNTHESIZED MAMMALIAN DNA IS RAPIDLY ASSEMBLED INTO CHROMATIN SUBUNITS PRIOR TO JOINING AT LOW MOLECULAR WEIGHT REPLICATION INTERMEDIATES. C.E. Hildebrand and R.A. Walters, Cellular and Molecular Biology Group, Los Alamos Scientific Laboratory, University of California, Los Alamos, New Mexico 87545

Current models for the structure of eukaryotic chromatin suggest a generalized repeating subunit structure in which histone octamers are associated with DNA at 200 base pair intervals. Chromatin replication requires synthesis of histone and nonhistone proteins and association of these proteins with newly replicated DNA. In eukaryotes, DNA is synthesized as low molecular weight intermediates ("Okazaki fragments," ~4S in denaturing sucrose gradients) which are subsequently joined to form continuous daughter DNA strands. We have examined (1) the kinetics of "Okazaki fragment" synthesis and maturation with higher molecular weight DNA strands and (2) the incorporation of newly synthesized DNA into chromatin subunits. In these studies, Chinese hamster cells (line CHO) were uniformly labeled with ^{14}C-thymidine and pulse-labeled for 0.5 min with ^{3}H-thymidine. Analysis of DNA from pulse-labeled cells shows that most of the newly synthesized DNA sediments at ~4S. Staphylococcal nuclease digestion of chromatin in intact nuclei isolated from pulse-labeled cells and subsequent analysis of the digested chromatin in isokinetic neutral sucrose gradients indicate a greater susceptibility to nuclease attack of chromatin subunits near the replication fork. This greater nuclease susceptibility of newly replicated chromatin is due to the organization of chromatin proteins on the DNA and not to properties of the newly synthesized DNA, as shown by experiments with isolated DNA. These results suggest that newly synthesized DNA is rapidly assembled into chromatin subunits before the 4S "Okazaki fragments" are joined. (This work was performed under the auspices of the U. S. Energy Research and Development Administration.)

F-AM-D10 REASSOCIATION KINETICS OF DNA PREFERENTIALLY PURIFIED BY DNA BINDING NONHISTONE PROTEIN FRACTIONATION. L.L. Jagodzinski‡ and J.S. Sevall, Chemistry Department, Texas Tech University, Lubbock, Texas 79409

Analysis of the DNA binding properties of the NHC-proteins from rat liver have indicated a class of moderate binding NHC-proteins (12.1% of the total NHC-proteins) are present which can interact preferentially with rat DNA[1,2]. Fractionation of the rat genome is possible by removal of protein bound DNA fragments that are retained on nitrocellulose filters. At protein to DNA mass ratios of 3:1, 20% Eco RI restricted rat DNA is isolated as protein bound DNA. In vitro labeling with DNA polymerase I and shearing restricted fragments to 350bp size allowed DNA reassociation kinetics to be followed. Second order reaction curves were fit to individual components of each reassociation curve. The bound DNA was represented by three components: 19.1% reassociating very fast, 33.1% reassociating with a $Cot_{1/2}$ of 0.0585, and a slow component of 40.3% with a $Cot_{1/2}$ of 588.2. The total rat DNA sequences are comprised of four components: a fast (9%), two moderate components (17.6% of $Cot_{1/2}$ 0.93 and 12.2% of $Cot_{1/2}$ 145), and a slow component (58.1%; $Cot_{1/2}$ 2460). The unbound DNA shows similar reassociation components as total rat DNA. DNA excess reassociation of total rat DNA and trace amounts of labeled bound DNA indicate we have enriched for sequences that are rapidly reassociated and moderate repetitive DNA sequences in the fast component of intermediate repetitious sequences. These results suggest that a class of rat liver NHC-proteins can interact with a subset of DNA sites which can be isolated for further analysis of protein-DNA interactions.

Supported by: National Science Foundation BMS-75-09232 and USPHS DHEW-NIH-GM-22653

1) L.L. Jagodzinski, J. Chilton, J.S. Sevall, Biophysical Journal, 16, 225a (1976).
2) J.S. Sevall, J. Chilton, L.L. Jagodzinski, M. Savage, Biophys. Biochim. Acta, in press

F-AM-D11 PROTON MAGNETIC RESONANCE, CIRCULAR DICHROISM AND RAYLEIGH SCATTERING STUDIES OF INTERACTION BETWEEN MONONUCLEOTIDES AND MODEL PROTEINS. J.C. Howard*, A.B. Cheung*, and H.J. Li (Intr. by A.G. Harford. Division of Cell and Molecular Biology, State University of New York at Buffalo, Buffalo, New York 14214.

The Rayleigh scattering of random copoly (Lys^{58}, Phe^{42}) or random copoly (Lys^{50}, Tyr^{50}) in aqueous solution was greatly enhanced by the binding of AMP or GMP but not by CMP or UMP. Proton magnetic resonance (PMR) spectra obtained for AMP, GMP, CMP or UMP individually as well as complexed with poly (Lys^{58}, Phe^{42}) indicated that severe line broadening and intensity loss occurred in the mixture of poly (Lys^{58}, Phe^{42}) with AMP or GMP but not with CMP or UMP. Both Rayleigh scattering and PMR results suggest a stronger binding to the model proteins by purine than by pyrimidine mononucleotides. In other words, stacking with aromatic tyrosine or phenylalanine residues is much stronger for purine than pyrimidine nucleotides. Circular dichroism (CD) spectra of these mixtures further indicated that poly (Lys^{58}, Phe^{42}) underwent a conformational transition from an unordered coil to a state which includes some α-helical and β-sheet structure the quantity of which is greater in the mixture with AMP or GMP than with CMP or UMP. (Supported by NIH grant GM 23079).

F-AM-D12 INDUCED RAYLEIGH SCATTERING OF NUCLEIC ACIDS BOUND BY PROTEINS AND ITS APPLICATIONS. H.J. Li, J.C. Howard*, M.L. Shiffman* and J. Tricoli*, Division of Cell and Molecular Biology, State University of New York at Buffalo, Buffalo, New York 14214.

The Rayleigh scattering intensity of both DNA and some RNA was increased by ten to one hundred fold when they were bound by polylysine, polyarginine or some other model proteins. The scattering intensity of the nucleic acids was increased when more nucleotides were bound and the intensity of a given complex was increased linearly as a function of the concentration of the complex. Digestion of the polypeptides in the complexes into oligopeptides by trypsin led to a drastic decrease of the Rayleigh scattering intensity. Thus increased Rayleigh scattering was induced when nucleic acids were tightly bound by proteins. Dissociation of proteins from DNA caused a drastic decrease of scattering intensity. Salt induced dissociation of polylysine (or polyarginine) from DNA was examined by Rayleigh scattering and was found to be independent of the G+C content of the DNA but depends upon the type of salt in solution. The induced scattering was also used to measure competition between single- and double-stranded RNA for polylysine binding. The results showed that poly(A)·poly(U) was favored over poly A and poly(I)·poly(C) was favored over poly I. This conclusion was confirmed by thermal denaturation experiments. (Supported by NIH GM 23079 and 23080).

F-AM-D13 THE CONDENSATION OF PURE DNA INTO QUASI-BIOLOGICAL STRUCTURES AFTER SIMPLE CHARGE NEUTRALIZATION AND DEHYDRATION OF THE POLYELECTROLYTE. T.H. Eickbush* and E.N. Moudrianakis, Biology Dept., Johns Hopkins Univ., Baltimore, Md. (intr. by R.C. Huang).

To better understand the structural consequences of nucleic acid - protein interactions, a systematic study was undertaken to analyze the effect of ionic strength and dielectric constant upon the conformation of pure DNA in solution and during its deposition on the carbon film of electron microscope grids. We found that pure DNA is loosely adsorbed onto the carbon film and collapses into a variety of structures after the grid is immersed in 95% ethanol. The exact structures that result from this dehydration were found to depend upon the ionic strength of the DNA solution, and thus reflected the degree of DNA phosphate charge shielding. DNA deposited from solutions of low ionic strength gave rise to supercoiled fibrillar structures in which the DNA is compacted linearly 8.5 fold. When deposited from solutions of intermediate ionic strength, the DNA collapsed in a non-uniform way, resulting in fibers with a "beads-on-a-string" appearance and a 150-Å diameter at the bead. This type of packing indicated that short regions of the DNA molecule collapse independently of one another. At ionic strengths sufficient to neutralize the DNA charge, folded-fiber structures appeared, represented by rod or toroidal forms. The significance of the similarities of these artifactually derived structures to those reported for DNA when compacted in chromatin or within the phage head will be discussed. We propose that the DNA double helix contains the necessary information to direct its own packaging into biological structures. The regulation of this intrinsic property is accomplished by controlling the neutralization and dehydration of this fibrillar polyelectrolyte.

F-AM-D14 A MODEL FOR CHROMATIN STRUCTURE: A SUPERCOILED, CHARGE-NEUTRALIZED POLYELECTROLYTE. E.N. Moudrianakis, T.H. Eickbush*, and R.L. Rubin*, Biology Department, Johns Hopkins University, Baltimore, Maryland 21218.

Studies with isolated chicken embryo chromatin and chromatin from calf thymus indicate that the DNA in native chromatin is differentially compacted. The highly compacted areas, with a packing ratio of ca. 6:1, represent areas not transcribable by exogenous polymerase, while the relaxed areas, with a packing ratio of $<3:1$, are transcribed under the same conditions. Viscosimetric and electronmicroscopic observations support the view that the basic structure of the chromatin fiber is a supercoil. Results from reconstitution studies indicate that histone-DNA interactions generate this supercoil and that the histone pair H3-H4 is the basic unit in stabilizing this supercoil (1). Although histones H2A and H2B contribute significantly to the overall structure of chromatin, they are of secondary importance in the stabilization of the supercoil. A model for chromatin structure will be presented which differs significantly from current views, but is in harmony with all the available direct experimental evidence. The physical parameters of the supercoil essential to this model will be described. Certain experimentally testable predictions derived from the model will be presented. These offer a basis for explaining differential gene expression and perhaps the regulation of DNA replication within eukaryotic chromosomes.

(1) R.L. Rubin and E.N. Moudrianakis, *Biochemistry 14*:1718 (1975).

F-AM-D15 CHROMATIN SUBUNITS, A STRUCTURAL MODEL R. D. Blake and James S. New*, Dept. of Biochemistry, University of Maine, Orono, Me. 04473.

Chromatin subunit monomers produced by staph-nuclease digestion of calf thymus nuclei, and containing DNA of 150 $\pm$ 15 base pairs in ionic association with H2A, H2B, H3 and H4, have been purified by isokinetic sucrose gradient centrifugation. Various chemical and physical properties of these subunits are identical with those of recent literature descriptions of subunits from a half dozen other species. The base composition and sequence of DNA in chromatin and chromatin subunit were found to be identical by quantitative analyses of sensitive derivative-absorption melting curves, obtained directly from a double beam, ratio recording spectrophotometer by maintaining ($\pm$ 0.008°) a small temperature differential between two identical solutions of DNA. Studies of the binding of actinomycin D indicate that one-half as many binding sites exist on the subunit as on free DNA, while chromatin has only one-third as many; yet the strength of binding to all three lattice systems is identical. The significance of these results will be discussed in the context of a dynamic model for chromatin structure. (Supported by grants from MAES, Project #315 and NIH, GM 22827)

F-AM-D16 IN VITRO TRANSCRIPTION OF HEAT SHOCK INDUCED GENES FROM DROSOPHILA MELANOGASTER CHROMATIN. H. Biessmann*, B. Levy W.*, and B.J. McCarthy,* Dept of Biochemistry & Biophysics University of California, San Francisco, Ca. 94143 (Intr. by H.J. Burki)

Heat inducible puffs appear at specific sites on the polytene salivary gland chromosomes in D. melanogaster shortly after raising the temperature from 25°C to 37°C. These puffs are transcribed in vivo and produce new RNA species not present in normal cells. In our experiments the heat shock triggered alterations in gene expression were used to study changes in chromatin template activity. The RNA synthesized after heat shock was isolated from polysomes of D. melanogaster cultured cells and used as template to prepare complementary DNA (cDNA). An excess of poly(A) RNA from heat shocked cells hybridized to 80% of the cDNA probe, whereas only 40% could be driven into hybrids by an excess of cytoplasmic poly(A) RNA from cells grown under normal temperature conditions. These latter sequences were removed from the cDNA population by complete annealing to poly(A) RNA from cells grown at 25°C and subsequent chromatography on hydroxylapatite. The unreacted material represents only heat shock induced mRNA sequences as shown by a second cycle of hybridization. Isolated chromatin was transcribed in vitro with E. coli RNA polymerase using mercurated UTP as precursor. Hg-containing RNA, free of DNA and endogenous RNA was purified by affinity chromatography on sulfhydryl-Sepharose 6B. RNA transcribed at 25°C from chromatin which was prepared from cells 1 hr after shifting the temperature to 37°C hybridized with a 100-fold faster kinetics to the heat shock specific cDNA probe than RNA transcribed from chromatin of cells grown at 25°C. We conclude that the in vitro transcription products of D. melanogaster chromatin with E. coli RNA polymerase reflect the functional state of the cell before isolation.

F-AM-E1 STEREOCHEMISTRY OF ETHIDIUM BINDING TO DOUBLE-HELICAL RNA. Chun-che Tsai, Department of Chemistry, Kent State University, Kent, Ohio 44242

X-ray crystallographic studies of two ethidium: dinucleoside monophosphate crystalline complexes (ethidium: 5-iodo-rU-rA and ethidium: 5-iodo-rC-rG) have allowed the direct visualization of drug intercalation into miniature Watson-Crick-type double helices at atomic resolution. Based on the stereochemical information afforded by these studies, a detailed molecular model for ethidium binding to double-helical RNA has been advanced. The model predicts that at maximal drug-nucleic acid binding ratios ethidium intercalates between every other base-pair in double-helical RNA (i.e. a neighbor exclusion model for intercalation). This follows from the mixed sugar puckering, C3' endo (3'-5') C2' endo, that is observed in the crystalline complexes. Base-pairs in the immediate region of intercalation are twisted by about 10^{o}; this gives an angular unwinding of -23^{o} for RNA intercalation. The intercalated base-pairs are also tilted relative to one another by about 8^{o} and form a V-type notch which opens from the narrow groove. The phenyl- and ethyl- groups of the ethidium molecule lie in the narrow groove of the double helix; this suggests that the direction of entrance by this drug is from the narrow groove of the double helix. A weak pyrimidine-purine sequence binding preference is predicted from stacking consideration of ethidium on adjcent base-pairs, as suggested by solution studies of ethidium-dinucleoside monophosphate interactions. Symmetry is utilized in the interaction, the approximate two-fold symmetry of the phenanthridinium ring system on ethidium coinciding with the two-fold symmetry of double-helical RNA at the intercalation site. A detailed sequence of conformational changes leading to drug-nucleic acid intercalation will be described at the meeting.

F-AM-E2 THREE DIMENSIONAL STRUCTURE OF E. COLI INITIATOR $tRNA_f^{met}$ AT 6Å RESOLUTION. N. H. Woo* and A. Rich, Biology Department, Massachusetts Institute of Technology, Cambridge, Mass. 02139

Highly ordered crystals of the E. coli initiator tRNA ($tRNA_f^{met}$) have been obtained. The molecule crystallizes in the orthorhombic space group $C222_1$, with cell dimensions a = 32Å, b = 84Å, c = 240A. The X-ray diffraction pattern of the crystal extends to an interplanar spacing corresponding to 3Å resolution. A low resolution 6Å data set has been collected on a diffractometer, and a 4.5Å data set including some 3Å data has been collected using oscillation methods. A full 3Å data set is being collected at present. We have used the yeast $tRNA^{phe}$ structure as a model in a rotation and translation function search. Initial results of these searches using the 6Å data have yielded as the best solution an orientation which is consistent with the packing constraints imposed by the crystal symmetry. These results are currently being further analyzed. This initial solution implies that at low resolution, the diffraction data from the $tRNA_f^{met}$ crystal is compatible with the overall conformation of the yeast $tRNA^{phe}$ structure. It is likely that any differences between the structures of the two molecules will become apparent when the higher resolution data is included in the analysis of the structure of the $tRNA_f^{met}$ molecule.

F-AM-E3 THEORETICAL CALCULATIONS OF CONFORMER PREFERENCES IN α-3'-5'-CYCLIC NUCLEOTIDES. R. Tewari, and S. S. Danyluk, Division of Biological and Medical Research, Argonne National Laboratory, Argonne, Illinois 60439

A comparative study has been made of configurational effects on conformational properties of α- and β-anomers of 3'-5' cyclic purine and pyrimidine nucleotides and 2'-arabino epimers. Correlations between the orientations of the base and the 2'-hydroxyl group have been studied theoretically using the PCILO (Perturbative Configuration Interaction using Localized Orbitals) method. The effect of change in ribose puckering on the base orientation has also been investigated. The results show that steric repulsions and stabilizing effects of intramolecular hydrogen bonding between the base and the 2'-OH are of major importance in determining conformations of α-anomers and 2'-arabino-β epimers. For example, hydrogen bonding between 2'OH and polar centers on the base ring is clearly implicated as a determinant of *syn-anti* preferences, i.e., χ_{CN} value in all anomers. Moreover, barrier heights for interconversion between the latter conformers are sensitive to ribose pucker and 2'OH orientations, e.g., when base-ribose interactions are minimal the barrier is small and the *syn/anti* ratio approaches unity. The calculations also show that ribose ring pucker plays an essential role in relieving repulsive interactions between the base and 2'-hydroxyl group. Thus a C3'-*endo*-C2'-*exo* ($^{3}_{2}T$) pucker is favored for α-anomers in contrast with the C4'-*exo*-C3'-*endo* ($_{4}T^{3}$) form found in β-compounds.

Acknowledgment: This research was supported by the U.S. Energy Research and Development Administration.

F-AM-E4 PROTON MAGNETIC RESONANCE STUDIES OF THE α-ANOMERS OF (3',5')-CYCLIC NUCLEOTIDES. CONFORMATIONAL ANALYSIS. M. MacCoss,* F. S. Ezra, and S. S. Danyluk, Division of Biological and Medical Research, Argonne National Laboratory, Argonne, Illinois 60439

A conformational study has been made of the α-anomers of 3',5'-cyclic nucleotides: 3',5'-cαAMP, 3',5'-cαUMP, and 3',5'-cαCMP. Proton NMR spectra were recorded for all of the compounds at 220 MHz and complete sets of chemical shifts and vicinal proton-proton and proton-phosphorus coupling constants derived for each compound. Due to the complexity of the spectra, lanthanide ion shift reagents were used to increase chemical shift separations between resonances. Conformational properties of the (3',5')-cyclic α nucleotides are not perturbed significantly in the presence of these reagents. Analysis of homo- and heteronuclear couplings shows that the cyclophosphate ring for all three compounds is locked into a chair form. The furanose rings, on the other hand, all show a preference for $_2T^3$-$^3T_2$ pucker, in contrast with the β anomers which favor ^3E-$_4T^3$. This change in furanose conformation can be attributed to a repulsive interaction between the 2'OH and base moieties. Implications of the conformational differences of α- and β-anomers will be discussed in regard to biological function.

Acknowledgment: This work was supported by the U.S. Energy Research and Development Administration.

F-AM-E5 PROTON MAGNETIC RESONANCE STUDIES OF THE PHOTOHYDRATION OF RIBODINUCLEOSIDE MONOPHOSPHATES. CONFORMATIONAL PROPERTIES OF ADENYLYL-(3',5')-6-HYDROXYDIHYDROURIDINE (ApU*) and 6-HYDROXYDIHYDROURIDYLYL-(3',5')-ADENOSINE (U*pA). F. S. Ezra, M. MacCoss,* and S. S. Danyluk, Division of Biological and Medical Research, Argonne National Laboratory, Argonne, IL 60439

The products of UV photoirradiation of ApU and UpA in aqueous solution have been identified and their structures determined by proton magnetic resonance spectroscopy at 360 MHz. Ultraviolet irradiation results in the hydration of the uracil base with OH addition occurring at C6 only. No "damage" can be detected at either the adenine base, ribose rings, or phosphodiester backbone under conditions of the experiment (T ∿ 0°C, pH - 7). The rate of hydration of the uracil base is significantly slower in the dimers as compared with 3'-UMP and 5'-UMP. Two isomers of the hydrated dimers, ApU* and U*pA, were indicated by the appearance of two sets of base and ribose ring pmr signals for each nucleotidyl fragment. Key structural features such as ribose ring conformation, exocyclic group rotamer populations, and relative base ring orientations have been deduced for each isomer from chemical shifts and vicinal proton-proton and proton-phosphorus coupling constants. The results demonstrate that significant changes occur in the conformational properties of the dimers upon photohydration. For example, the ribose ring $^2E \rightleftharpoons {}^3E$ equilibrium shifts on the average from 55% ^3E to 55% ^2E and the phosphodiester backbone adopts an increasingly extended configuration.

Acknowledgment: This research was supported by the U.S. Energy Research and Development Administration.

F-AM-E6 FLUORESCENT PROBE CONFORMATIONS. THE CRYSTAL STRUCTURE OF MAGNESIUM AND AMMONIUM ANS. Vivian Cody and John Hazel*, Medical Foundation of Buffalo, Buffalo, New York 14203

Fluorescent probes of the ANS (8-anilino-1-naphthalenesulfonic acid) type have been extensively used to explore the binding sites of substrates, enzymes, membranes and proteins. While the mechanism of fluorescent enhancement is not clearly understood, a coplanar conformation of the two rings is a suggested prerequisite. Solution NMR studies also suggest that an intramolecular hydrogen bond stabilizes the coplanar conformation. The crystal and molecular structure of the magnesium and ammonium salts of ANS have been determined. The magnesium salt (ANS·1/2 $(Mg(H_2O)_6)\cdot 3H_2O$) has a coplanar conformation as indicated by the anilino nitrogen geometry with torsion angles C6'-C1'-N-C1 = 174° and C1'-N-C1-C2 = -54°, an intramolecular N-H...O hydrogen bond and close H...H intramolecular contacts. The ammonium salt $(2(ANS\cdot NH_4)\cdot H_2O)$ has two distinct conformations, one with a coplanar nitrogen (torsion angles 171°/-46°) and the other with a tetrahedral nitrogen (112°/22°). Both molecules have the same intramolecular hydrogen bonds, in contrast to the solution NMR results, and the same close H...H intramolecular contacts. The hydrogen intramolecular contacts in all three molecules are made by the same hydrogens which give rise to anomalous proton NMR signals. These observations may represent discrete energy minima for the fluorescent probe and could be important to the understanding of their fluorescence mechanisms.

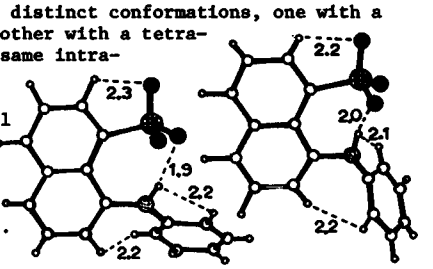

Supported by NIH grant AM15051.

F-AM-E7 THE THREE DIMENSIONAL STRUCTURE OF A SNAKE VENOM NEUROTOXIN. Demetrius Tsernoglou* and Gregory A. Petsko*, Biochemistry Department, Wayne State University Medical School, Detroit, MI 48201. (Sponsored by Robert A. Mitchell).

The complete structure of a post-synaptic neurotoxin from the venom of sea snake Laticaude semifasciata has been determined by x-ray crystallography at 1.38 Å resolution. All atoms have been located and the structure has been refined. The molecule is a disc with three main loops of anti-parallel β-pleated sheet extending from a core built around four disulfides. We believe all α-neurotoxins including α-bungarotoxin and cobrotoxin have essentially the same structure. A model will be discussed for the interaction of such toxins with the acetylcholine receptor. The structure has also led us to a hypothesis about the mode of action of cardiotoxin. (Supported by USPHS grant No. HL-15958-04).

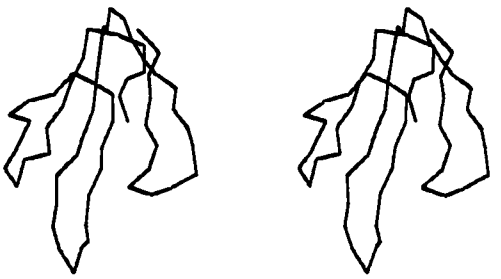

F-AM-E8 SIDE CHAIN MOBILITY AND THE CALCULATION OF TYROSYL CIRCULAR DICHROISM OF PROTEINS. A. Wollmer†, J. Fleischhauer†, and W. Strassburger†Technischen Hochscule, Aachen, Germany, and Dan Mercola and G. Dodson† Dept. Zoology, Oxford, England.

The tyrosyl circular dichroism (CD) of insulin has been calculated (1) using the monopole approximation of Woody (2) and the crystal structure coordinates taking into account all peptide bonds and side chains of His, Arg, Asn, Gln, Asp, Glu, Phe, and Tyr. The results (essentially at 0°K) explain about 70% of the observed (298°K) CD. The calculations show that the most important sources of Tyr CD are other nearby aromatic groups. We have now tested this relationship by removing the terminal B-1 Phe of insulin which causes the largest (40%) effect due to proximity to A-14 Tyr. In contrast to expectation, the measured values for insulin and the despheinsulin over a wide range of concentrations with/out zinc are very similar. Recent crystal structure refinement results have revealed that the B-1 Phe (a surface residue) is unusually mobile ($\bar{B}$ = 35). Calculations using the crystallographic temperature factors (B values) show that this disorder will reduce expected CD values for ring separations up to 4 Å and qualitatively accounts for the overestimated CD for the B-1 - A-14 interaction. Quantitative calculations are in progress. (1) E.H. Strickland, and Dan Mercola, Biochemistry, 15, 3875 (1976). (2) R. Woody, J. Chem. Phys., 49, 4797 (1968).

F-AM-E9 STUDIES ON THE CHROMOPHORIC SIDECHAINS OF RABBIT TROPOMYOSIN. Bela Nagy, Dept. of Muscle Research, Boston Biomedical Res. Inst., 20 Staniford St., Boston, MA 02114

Recent studies have shown a strong negative circular dichroic band (CD) in the tyrosine region of tropomyosin (TM) (Chao and Holtzer, Biochemistry 14, 2164, 1975). This strong CD effect and the anomalous shape of the band have been attributed to tyr-tyr interactions (Bullard et al., Biochim. Biophys. Acta 434, 90, 1976). We have found that not only tyr but also phe chromophores are optically active in TM and their CD is reduced on denaturation, an effect which is consistent with the rigidity imposed on sidechains in the α-helical form. Changing the pH from 7.5 to 2 has no effect on the α-helix content but the anomalous shape of the tyr CD spectrum disappears without a reduction in its magnitude and the fluorescence of tyr increases. The latter effect is in contrast to the quenching effect of protons on simple tyr compounds. The tyr fluorescence behavior of TM is consistent with COO^- quenching at pH 7 or, possibly, with hydrogen bonds between tyr and glu sidechains in the native helical form. In denatured TM lowering the pH quenches the fluorescence. Dityrosines, involving the ortho position, linking the two subunits in TM can be formed by peroxidase mediated oxidation or by UV irradiation. This proves that the tyr residues in TM are between the interacting subunits as suggested by other data (Nagy, 9th Meeting FEBS, Abstr. p. 21, 1974). In model compounds dityrosine is formed only between tyrosinates. Since in TM dityrosines are formed even at pH 8, the increased reactivity is likely to be due to the hydrogen bonds postulated above. (Supported by grants from NSF, BMS 7516140, and NIH, HL5949.)

F-AM-E10 A COMMENT ON THE INTERPRETATION OF INFRARED LINEAR DICHROISM MEASUREMENTS ON ORIENTED NUCLEIC ACID FILMS. C.P. Beetz,Jr. and G. Ascarelli, Physics Dept. and S. Arnott, Biology Dept., Purdue University, West Lafayette, Indiana 47907

Recent measurements of the i.r. linear dichroism spectra of oriented nucleic acid films[1] have been used to define the orientation of the phosphate group in the backbone of the nucleic acid molecule. These results are in disagreement with the findings of x-ray diffraction measurements[2]. The previous interpretation of the i.r. data is based on the assumption that the vibrations of the phosphate group are weakly coupled to those of the rest of the molecule. The motions of the two unesterified oxygen atoms can then be considered to be either in phase or 90° out of phase. Neither the assumption nor the conclusion are valid because the phosphate group is an integral part of the nucleic acid backbone and participates in all the normal modes of the backbone as well as the localized phosphate vibrations. Finally the binding of the phosphate group in the backbone of the molecule destroys the symmetry necessary for the simple classification of the oxygen motions as in phase or out of phase. The results of several recent normal mode calculations[3] verify this fact. A calculation is presented in which the i.r. data is interpreted using the results of a detailed normal mode calculation for the nucleic acid backbone. The results of this interpretation bring the i.r. data into better agreement with the x-ray diffraction results. (Supported in part by NIH grant GM00779.)

1. J. Pilet and J. Brahms , Biopolymers 12, 387 (1973).
2. S. Arnott and D.W.L. Hukins, B.B.R.C. 47, 1504 (1972).
3. J.M. Eyster and E.W. Prohofsky, Biopolymers 13, 2527 (1974).

F-AM-E11 ELECTRON NUCLEAR DOUBLE RESONANCE (ENDOR) OF HEMINS. C. P. Scholes, H. L. Van Camp‡ and C. F. Mulks‡ Department of Physics, SUNY/Albany, Albany, N. Y. 12222

ENDOR and EPR signals were obtained from deuterohemin† and protohemin dimethyl esters. With magnetic field along the symmetry axis of the heme, we detected magnetic hyperfine interactions from heme nitrogens, protons, and heme axial ligands (F^-, Cl^-, Br^-). Hemin compounds were frozen in the following solvent systems which hinder hemins from self-aggregation and which do not replace the desired axial anion on heme: (1) a 1:1 mixture of $CHCl_3$-CH_2Cl_2 that contained a 5-fold molar excess (relative to hemin) of diamagnetic, metal-free porphyrin; (2) a 1:1 mixture of THF-$CHCl_3$. Hemin anions were varied in the following series which is in the order of decreasing metal-ligand bond strength: fluoride, formate, acetate, azide, chloride, and bromide.

Nitrogen ENDOR. With solvent kept constant, differences of a few percent in nitrogen hyperfine couplings were seen between heme compounds with different axial anion. There were no clear trends in nitrogen couplings as a function of axial anion. The nitrogen couplings were significantly higher for all compounds in $CHCl_3$-CH_2Cl_2 than in THF-$CHCl_3$.

Proton ENDOR. In $CHCl_3$-CH_2Cl_2 we saw a systematic (~6%) increase in heme meso proton couplings resulting from the change of heme axial anion from fluoride through bromide. This increase is highly consistent with meso proton changes seen by NMR on the same hemin compounds. In THF-$CHCl_3$ very little change was seen from the meso protons due to change of heme's axial anion. However, ENDOR showed that THF protons do interact with the hemins.

(This work supported by NIH Grant No. AM-17884.)

†Deuterohemin esters werekindly provided by Prof. W. S. Caughey.

F-AM-E12 DETECTION AND EXAMINATION OF DENSE BODIES IN HYDRATED HUMAN PLATELETS. J.L. Costa*, S.W. Hui, C.M. Strozewski*, Y. Tanaka*, and M.A. Smith*. NIMH, NIH, Bethesda, MD 20014; Electron Optics Lab., Roswell Park Memorial Institute, Buffalo, NY 14263; and Division of Health Affairs, Univ. of No. Carolina, Chapel Hill, NC 27514.

Human platelets have been maintained in a hydrated state while photographed in an electron microscope, utilizing the temperature-controlled, open-window hydration chamber developed previously (Nature 262:303, 1976). Dense bodies (DB) are easily distinguishable, and their morphology and distribution in platelets resuspended in plasma or a sodium-chloride-Tris-citrate buffer parallels that seen in air-dried whole mounts (Science 183: 537, 1974). Serial photographs reveal no detectable movement or loss of DB over a 5-minute period. Platelets photographed, removed from the microscope, treated with thrombin, and then photographed again, have fewer DB following the thrombin treatment than before. Similarly, platelets treated with thrombin at 4°C, photographed at 4°C, and then photographed during warming to 25°C, lose DB during the warmup process. The following conclusions seem warranted: (1) The DB seen in air-dried whole mounts are not likely to be drying-related artifacts; (2) DB in unstimulated platelets may be anchored in such a fashion as to prevent Brownian motion; (3) Platelets appear to be capable of a secretory response to thrombin after exposure to the electron beam, and therefore probably survive under the conditions prevailing in the hydration chamber. This work is supported in part by NIH (CA-15330) to S.W. Hui who is also a Career Development Awardee (CA-00084).

F-AM-E13 FINE STRUCTURE AND INTERNAL ORGANIZATION OF THE ZYMOGEN GRANULE. T.H. Ermak* and S.S. Rothman, Department of Physiology, University of California, San Francisco, CA 94143

The zymogen granule of the pancreatic acinar cell probably contains as many as 20-30 distinct proteins in ordered association with each other and undefined structural moieties. Unfortunately, these secretory granules ($\bar{x}$ diameter ∿0.86 μm) have a relatively homogeneous, electron dense interior whose structural organization is not readily revealed in tissue sections. We attempt to overcome this difficulty by examining 1) dissociated zymogen granule contents, 2) granule material reassociated with granule membrane, and 3) granules partially depleted of their contents by dilution. Zymogen granule contents which are released into solution (at pH 8.6) and negatively stained with PTA form 50-400 Å particles (∿300 Å predominating). They contain ∿50 Å subunits, often aligned in rows, which probably are individual or small groups of protein molecules. When the particles are reassociated with granule membrane (at pH 5.5), an electron dense reticular meshwork is seen in thick sections (∿0.5 μm); this material contains virtually all the released enzyme. The reticular strands frequently form 120° angles with each other and make point attachments on the membrane; occasionally, complete hexagonal rings (∿0.3 μm across) are produced. At appropriate dilutions of whole zymogen granules, large numbers of reticulated granules can be produced from electron dense precursors. They also contain strands of electron dense material which here outline spherical and polygonal spaces (∿0.1-0.3 μm) and attach to granule membrane; 120° angles between strands suggest hexagonal units. Thus, digestive enzymes, probably in association with structural molecules, form an intragranular reticulum which attaches to granule membrane at discrete sites and can be spontaneously disassembled into multimolecular particles and then reassembled in association with granule membrane as a function of pH. (Supported by NIH grants AM05407 and AM16990).

F-AM-E14 INTERCELLULAR BRIDGES IN TWO HORMONALLY-RESPONSIVE CELL LINES DEMONSTRABLE AFTER STAINING FOR MUCOSUBSTANCES. Edward Siegel, Radiation Biology, Department of Radiology, Vanderbilt University School of Medicine, Nashville, Tenn. 37232.

Two cell lines strongly responsive to hormones and cell-cell dependent, the T-1 human kidney and the steer thyroid lines, possess intercellular bridges that are demonstrable after staining for mucosubstances with alcian blue. As reported previously, the T-1 cells are sensitive to and specific for the thyroidal hormones and related amino acids in influencing dimensions, morphology, and metabolism. Even after months of serial propagation, the cultured steer thyroid line has been shown to preserve aspects of differentiation as indicated by parameters reflecting cellular proliferation and function which are affected by thyrotropin (TSH) or the long-acting thyroid stimulator (LATS). Both cell lines were grown as monolayers and maintained at 37 C in water-saturated incubators gassed with a 95% air-5% CO_2 mixture; the growth medium used was Eagle's MEM with fetal bovine serum (10%) and penicillin-streptomycin. After fixing, cells were stained with periodic acid Schiff-alcian blue at pH 2.5. Under the microscope these intercellular bridges are seen to consist of multiple, wavy strands; they are not co-planar and vary greatly in length. Many of these links apparently connect the nucleus of one cell to the cytoplasm of a neighbor. In view of the special behavior exhibited by these cell lines, these threads rich in mucosubstances may prove important channels for intercellular interactions; the demonstration of these processes raises questions at least as to their ubiquity, function, and detection. These investigations were supported by a research grant from the John A. Hartford Foundation, Inc., New York.

F-AM-E15 SIZE DEPENDENCE OF PHASE TRANSITIONS AND RELEVANCE TO PLASMA LOW DENSITY LIPOPROTEINS. D. Armitage, G.G. Shipley, and D.M. Small, Biophysics Division, Boston University School of Medicine, Boston, MA. 02118.

The structure and thermodynamics of biological systems are often strongly influenced by size and surface effects. An example is the thermal transition in human plasma low density lipoprotein (LDL, a 200 Å diameter particle) at about body temperature. This broad transition was interpreted as the formation of a smectic liquid crystal phase by the cholesteryl ester (CE) component of the particle (R.J. Deckelbaum, et al., Science 190, 392 (1975)). Isolated LDL CE's exhibit a clearly defined cholesteric liquid crystal phase and show a sharp transition to the smectic phase. To study size effects we absorb CE in porous silica of uniform pore size (∿ 150 Å diameter) and observe the behavior of absorbed CE compared with bulk unabsorbed CE. Differential scanning calorimetry studies of absorbed CE show that the solid melting point is depressed by about 6°C and the liquid crystal transitions are depressed by about 1°C. All the transitions are broadened by several degrees resulting in the merging of the smectic and cholesteric peaks. The transition enthalpies decrease by about 50%. The observations in LDL, particularly the reduction in transition enthalpy, broadening and lack of a cholesteric peak, are similar to the size effects produced by pore absorption of CE. This indicates that features of the transition in intact LDL may be attributed to the limited domain size available to its CE.

F-AM-E16 STEM STUDIES OF SELECTIVELY LABELLED BOVINE PANCREATIC RIBONUCLEASE
L.T. Germinario*, J.W.Wiggins*, and M.Beer, Dept. Biophys. The Johns Hopkins University, Baltimore, Md. 21218

The interaction of five Pt complexes, K_2PtCl_4, K_2PtCl_6, DMSOPt,Pt(L-MetH)Cl_2 and [Pt(Gly-L-MetH)Cl] Cl, with bovine pancreatic ribonuclease-A(RNase-A) (E.C. 2.7.7.16) were investigated in order to prepare heavy atom derivatives which: (1) achieve quantitative and highly site-specific labeling, (2) react under mild (physiological) conditions, (3) yield a water soluble product, and (4) produce minimum distortion and perturbation tothe 3-D structure. Only chloro-glycyl-L-methioninatoplatinum (II) [Pt(Gly-L-MetH)Cl]Cl meets all the above requirements. A Job's plot at 251nm indicates that [Pt(Gly-L-MetH)Cl] Cl and RNase ($7.35X10^{-5}$M) react quantitatively to form a 3:1 complex which retains 60% of its former hydrolytic activity of cytidine-2',3'phosphate. Amino acid analysis, spectrophotometric difference spectra and thin layer chromatography implicate methionine as the reactive site. Preliminary results demonstrate the ability of the scanning transmission electron microscope (STEM) to image single Pt atoms covalently bonded to a protein molecule. Comparison of STEM micrographs of RNase molecules with light shadowgraphs of a 6A resolution balsam wood model of RNase-S reveal similarities in major features in the conformation of the RNase polypeptide chain. Supported by NIH GM08968, LTG supported by NIH 5FOGM57395. The 6A resolution balsam wood model of RNase-S was kindly loaned by H.W. Wyckoff.

F-AM-F1 PERMEABILITY OF THE THYLAKOID MEMBRANES TO INORGANIC ANIONS. P.H. Homann, Department of Biological Science and Institute of Molecular Biophysics, Florida State University, Tallahassee, FL 32303.

When DCMU poisoned isolated chloroplasts are illuminated in the presence of N-methylphenazinium methosulfate, N-methylphenazinium cations (MP^+) are taken up into the thylakoids. This uptake can be followed by observing the decrease of the absorption of MP^+ which is attributed to a "flattening" of the absorption by the heterogeneous distribution of MP^+ between medium and grana. Often as many as 7 MP^+/chlorophyll are taken up. However, the extent of the uptake is dependent on the concentration of membrane permeant anions in the medium. The rate of the uptake varies with the type of available anions in the following way: $Cl^- \approx Br^- \approx NO_3^- > SO_4^{2-} > Fe(CN)_6^{4-} \gg HPO_4^{2-} \approx F^-$. It is suggested that anions follow MP^+ into the thylakoids as counterions, and that their influence on the rate of MP^+ uptake reflects the permeability of the thylakoid membrane to the particular anion. The light dependent bleaching of MP^+ in the presence of chloroplasts, therefore, provides a rapid comparison of the relative permeabilities of thylakoid membranes to various anions. (Supported by a grant from the National Science Foundation)

F-AM-F2 THE PRIMARY LIGHT INDUCED EVENTS OF PHOTOSYNTHESIS AS REVEALED BY ANISOTROPIC ELECTRON SPIN POLARIZATION. I EXPERIMENTAL OBSERVATIONS. K.H.Sauer‡ R.E. Blankenship, G.C. Dismukes‡ and A. McGuire, Department of Chemistry and the Laboratory of Chemical Biodynamics, Lawrence Berkeley Laboratory, University of California, Berkeley, CA 94720.

The nascent populations of the electron spin energy levels of the oxidized reaction center of photosystem I, $P700^+$, from spinach chloroplasts are not in thermal equilibrium when observed promptly after light excitation. Examination of the Electron Spin Resonance (ESR) spectrum within a few microseconds following pulsed light excitation and prior to spin relaxation, indicates a marked dependence of the amplitude and shape of the $P700^+$ spectrum on the orientation of the radicals in the applied field of the spectrometer. This occurs despite the absence of appreciable magnetic anisotropy in the ESR spectrum of relaxed $P700^+$. All of the spectral features of the spin polarized $P700^+$ signal are accounted for by a radical pair mechanism in which the two neighboring radicals, produced upon photoionization of P700, undergo time dependent magnetic and exchange interactions. The anisotropy of the ESR spectrum of $P700^+$ prior to relaxation is due then to its interaction with the reduced primary electron acceptor, for which a large g-tensor anisotropy is indicated. The orientation studies indicate the Z component of the principal g-tensor for the primary acceptor lies in the plane of the thylakoid membrane. The ESR spectrum of the spin polarized primary acceptor is not observed at room temperature, suggesting it is efficiently relaxed. Complementary ESR studies of the photoreduced bound ferredoxins indicate no preferred orientation in the thylakoid membrane, implying neither center acts as the primary electron acceptor. The effect of chemical reduction of the ferredoxin centers will be discussed also.

F-AM-F3 THE PRIMARY LIGHT INDUCED EVENTS OF PHOTOSYNTHESIS AS REVEALED BY ANISOTROPIC ELECTRON SPIN POLARIZATION. II RADICAL PAIR THEORY OF MEMBRANE BOUND RADICALS. C. Dismukes‡ R. Friesner, and K. Sauer‡ Department of Chemistry and the Laboratory of Chemical Biodynamics, Lawrence Berkeley Laboratory, University of California, Berkeley, CA 94720

In a companion paper, it was shown that the electron spin populations of radicals produced upon photooxidation of the reaction center of photosystem I, P700, do not exist in thermal equilibrium immediately after charge separation. A model which predicts this behavior is proposed in which electron transfer from the first excited singlet state of P700 occurs to an acceptor molecule, possessing several sites between which the electron may be reversibly transferred, thereby modulating the electron spin exchange interaction of the partner radicals. Subsequent transfer to a secondary acceptor is considered as well. The proposed electron transfer dynamics agree with the properties observed for mixed valence complexes, which are models for the reduced acceptor molecule. The model indicates that spin polarization develops through the combined effect of the different Zeeman and hyperfine fields on adjacent radicals producing mixing of the singlet and triplet spin states of the pair, and the subsequent action of spin exchange, upon reencounter of the radicals, in producing the selective population of the spin states of the individual radicals. In the theory, both a time-dependent perturbation approach and a density matrix formulation including a Liouville operator for the electron transfer are considered. A calculated ESR spectrum for $P700^+$ is reported which agrees with a dimer chlorophyll structure possessing neglible g-value and hyperfine anisotropies. By considering a membrane bound acceptor molecule possessing an anisotropic g-tensor, all of the orientation dependent features of the experimental ESR spectrum of spin polarized $P700^+$ are reproduced in the calculated spectra. Information on the identity and orientation of the radicals in the photosynthetic membrane is obtained.

F-AM-F4 ALKALINE-UREA-DETERGENT SOLUBILIZATION AND COLUMN ELECTROPHORESIS SEPARATION OF PHOTOTRAP COMPLEXES FROM SPINICH CHLOROPLASTS. A. Das Gupta* and B. J. Hales, Department of Physics and Department of Chemistry, Louisiana State University, Baton Rouge, La. 70803.

Sonicated spinach chloroplasts have been subjected to the alkaline-urea-detergent treatment perfected by Loach and coworkers[1-3] for the dissolution of phototrap complexes from bacterial systems. In this treatment we have utilized three different detergent groups: 1) Triton X-100, 2) a Triton-SDS mixture and 3) LDAO. After each treatment the systems were neutralized, dialyzed and separated on a solution electrophoresis column. Of the three detergent systems, LDAO was found to produce an insufficient breakdown of the membrane structure to allow proper electrophoretic separation while TX-100/SDS appeared to produce a more complex membrane dissolution than TX-100 alone. None of the treatments was found to destroy system I photochemical activity. Results will be presented comparing the absorption spectra, polypeptide composition, esr spectra and back-electron transport kinetics of each of these systems.

1. P. A. Loach, D. L. Sekura, R. M. Hadsell and A. Stemer, Biochemistry, 9, 724 (1970).
2. P. A. Loach, R. M. Hadsell, D. L. Sekura and A. Stemer, Biochemistry, 9, 3127 (1970).
3. P. A. Loach and R. L. Hall, Proc. Nat. Acad. Sci., 69, 786 (1972).

F-AM-F5 A PHOTOSYSTEM I PHOTOVOLTAIC CELL. E.L. Gross and S.L. Winemiller*, Dept. of Biochemistry, Ohio State University, Columbus, Ohio 43210

We have developed a photovoltaic cell using Photosystem I-P700-chlorophyll a protein described by Shiozawa et al. [Arch. Biochem. Biophys. 165: 388 (1974)]. The protein is precipitated on a Metricel GA-6 filter, which is placed between two compartments containing the electron donor $[K_4Fe(CN)_6]$ and the electron acceptor (FMN) respectively. The filter area was 2 cm^2 and contained 0.03 mg chlorophyll. The filters could be stored refrigerated in a damp atmosphere and used repeatedly for at least three weeks. Maximum power was developed in 12 minutes and could be maintained for over 10 hours. Argon was bubbled through the system to maintain it in an anaerobic state. Optimum conditions consist of 20 mM Tris-Cl pH 7.6, 100 mM KCl, 2 mM $MgCl_2$, and either 10 mM $K_4Fe(CN)_6$ + 2mM $K_3Fe(CN)_6$ or 3mM FMN. Platinum electrodes were used. Saturating white light was used for illumination. Open circuit potentials ranged between 0.4 and 0.5 volts, negative on the FMN side. Maximum power was developed across a load resistance of 600 ohms, the corresponding voltage, current, and power being -0.33 V, 0.54 mamps, and 0.18 mwatts respectively. This corresponds to 0.89 watts/meter squared. The maximal current extrapolated to zero resistance was 1 mamp.

F-AM-F6 ENERGY DISTRIBUTION IN THE PHOTOSYNTHETIC APPARATUS OF HIGHER PLANTS. R. J. Strasser and W. L. Butler, Dept. of Biology, University of California, San Diego, La Jolla, California 92093.

Equations are derived from our model of the photochemical apparatus of photosynthesis to show that the yield of energy transfer from Photosystem II to Photosystem I, $\varphi_{T(II\rightarrow I)}$, can be obtained from measurements on an individual sample of chloroplasts frozen to -196°C by comparing the sum of two specifically defined fluorescence excitation spectra with the absorption spectrum of the sample. Then, given that value of $\varphi_{T(II\rightarrow I)}$, the fraction of the quanta absorbed by the photochemical apparatus which is distributed initially to Photosystem I, α, can be determined as a function of the wavelength of excitation from the same fluorescence excitation spectra. The results obtained in a study of spinach chloroplasts frozen to -196°C in the absence of divalent cations indicate that $\varphi_{T(II\rightarrow I)}$ varies from a minimum value of 0.10 when the Photosystem II reaction centers are all open to a maximum value of 0.25 when the centers are all closed and that α has a value of about 0.30 which is almost independent of wavelength for wavelengths shorter than 675 nm (α increases rapidly toward unity at wavelengths longer than 675 nm). These values agree quite well with results obtained previously from comparative measurements of chloroplasts frozen to -196°C in the presence and absence of divalent cations. These techniques have also been used to analyze the distribution of excitation energy in dark-grown bean leaves which have been partially greened by a series of brief flashes. Such leaves, which lack the light-harvesting chlorophyll a/b protein, show higher values of $\varphi_{T(II\rightarrow I)}$ than were found in spinach chloroplasts and a much more pronounced wavelength dependence of α across the visible spectrum.

F-AM-F7 FURTHER EVIDENCE FOR A PHOTOSYSTEM II-LINKED MEMBRANE CONFORMATIONAL CHANGE IN CHLOROPLASTS. L.J. Prochaska and R.A. Dilley, Department of Biological Sciences, Purdue University, West Lafayette, Indiana 47907.

The water-soluble chemical modification reagent, iodoacetic acid was used to monitor spinach chloroplast thylakoid membrane conformational changes. The incorporation of (^{3}H)-iodoacetate showed the following pattern: 1) There was an increased level of incorporation of iodoacetate in the light compared to dark or light plus DCMU conditions. A 30 to 50 percent increase in iodoacetate incorporation from about 1.0 moles per mg Chl to 1.3 to 1.5 moles per mg Chl was found; 2) The incorporation pattern indicated that Photosystem II electron transport and a functional water oxidation system were required to elicit the extra binding; a) Cyclic electron flow mediated by phenazine methosulfate in the presence of a Photosystem II inhibitor (DCMU) did not induce the extra binding of iodoacetate; b) In chloroplasts made deficient in water oxidation by NH_2OH treatment, electron flow from I^- to methyl viologen did not support the extra binding of iodoacetate; 3) Uncouplers of phosphorylation (nigericin plus valinomycin) did not affect the extra binding, suggesting that conformational changes in the coupling factor were not involved. The working hypothesis we suggest (c.f. Giaquinta et al., Biochemistry 14,4392 (1975) is that protons released from water oxidation are bound to fixed charge groups of certain membrane proteins, causing rearrangments in various membrane components. Protons translocated by the plastoquinone shuttle or by the artificial cyclic electron transport system do not interact with the component(s) involved in the photosystem II-linked conformational change. This work was supported in part by Grant GM 19595 from the N.I.H. and GB 30998 from the N.S.F., and a N.I.H. Career Development Award to R.A.D.

F-AM-F8 THE ROLE OF PLASTOQUINONE AND β-CAROTENE IN THE PRIMARY REACTION OF PLANT PHOTOSYSTEM II. D.B. Knaff, R. Malkin, J.C. Myron‡ and M. Stoller‡ Department of Chemistry, Texas Tech University, Lubbock, Texas 79409, and Department of Cell Physiology, University of California, Berkeley, California 94720.

Extraction of Triton Photosystem II chloroplast fragments with 0.2% methanol in hexane for 3 h results in the removal of 90 to 95% of the plastoquinone in the original preparation. The extracted fragments (chlorophyll:plastoquinone ratio, 900:1) showed no P680 photooxidation at 15°K after a single laser flash. The extracted fragments also showed no light-induced C-550 absorbance change at 77°K. Reconstitution of the primary reaction of Photosystem II, as evidenced by restoration of low-temperature photooxidation of P680, could be obtained by the addition of plastoquinone A but not by the addition of β-carotene. The addition of β-carotene plus plastoquinone A restored the C-550 absorbance change. These results indicate that plastoquinone functions as the primary electron acceptor of Photosystem II and that β-carotene does not play a direct role in the primary photochemistry but is required for the C-550 absorbance change. Supported in part by NSF Grants BMS-75-19736 and BMS 75-18879.

F-AM-F9 FLUORESCENCE YIELD RISE AND DELAYED LIGHT EMISSION DECAY IN THE 3-100 μsec TIME RANGE IN ISOLATED CHLOROPLASTS AFTER A SINGLE FLASH. P.A. Jursinic* and Govindjee, Department of Physiology and Biophysics, University of Illinois, Urbana, Illinois 61801.

The rise in chlorophyll *a* fluorescence yield and delayed light emission (DLE) decay, after a single 10 ns saturating excitation flash, have been studied in alkaline Tris-washed and NH_2OH treated chloroplasts. In dark-adapted samples, no Tris effect was observed; instead, as in the control, fluorescence yield rose exponentially with a lifetime of 6 μs and the DLE decayed with components having lifetimes of 6 and 30 μs. If two or more preillumination flashes were given at rates > 1 flash/s, then the fluorescence yield rose slowly to a value of $1.40\phi_o$ at 20 μs and the 6 and 30 μs DLE components were reduced while a 60-70 μs component was greatly enhanced. These data indicate that Tris has no direct effect on the $ZP^+_{680}Q^- \rightarrow Z^+P_{680}Q^-$ charge stabilization reaction. The effect of Tris is only observed when charge has built up on the oxygen side of Photosystem II and, since this requires two flashes--a capacity to hold two charges exists between the Tris block and P^+_{680}. The 6 and 30 μs components of DLE reflect the rapid charge stabilization steps on the oxygen side of Photosystem II. Conditions which led to a small rise in fluorescence yield [high (P^+_{680})] gave greatly enhanced DLE confirming the $P^+_{680}Q^-$ back reaction hypothesis. Donors (ascorbate, reduced phenylenediamine and benzidine) reversed the effects of Tris washing only if pre-illumination flashes were given at rates slower than the electron donation times of these components. Mn^{2+} is found to donate electrons to Z not directly to P^+_{680} because (1) in Tris-washed chloroplasts plus Mn^{2+}, the rise in fluorescence yield becomes 6 μs, identical to control; (2) in chloroplasts treated with 2 mM NH_2OH, which breaks the electron flow between Z and P_{680}, the addition of Mn^{2+} does not re-establish the rise in fluorescence yield.

F-AM-F10 CONCENTRATION-QUENCHING OF CHLOROPHYLL FLUORESCENCE: ANOMALIES. Vincent P. Gutschick* (Intr. by W. B. Goad), Theoretical Division, Los Alamos Scientific Laboratories, Los Alamos, New Mexico, 87545.

High concentrations of chlorophyll-*a* in ordinary solvents cause true quenching of fluorescence, yet none of the common mechanisms seem to apply. Neither ground- nor excited-state dimers (with cancelling radiative dipoles) are bound. Beddard and Porter [Nature 260, 366 (1976)] indicate that purely-statistical "dimers" at <10 Å separation probably effect the quenching. For these, increased intersystem crossing is unlikely, but a dissipative electron transfer may be demonstrable. Lifetime measurements would be quite helpful. *In vivo*, the values of fluorescent lifetime and yield imply only a competitive (trap) quenching and little or no concentration-quenching. The ordered, proteinaceous environment appears to enforce this and other means of protecting singlet excitations in the "antenna" systems.

F-AM-F11 INVOLVEMENT OF THE LIGHT-HARVESTING CHLOROPHYLL PROTEIN COMPLEX OF CHLOROPLASTS IN EXCITATION ENERGY DISTRIBUTION BETWEEN THE PHOTOSYSTEMS. Salil Bose*, J. R. Lieberman*, and C. J. Arntzen, Botany Department, University of Illinois, Urbana, IL 61801

Chloroplasts from a barley mutant containing no light-harvesting pigment protein complex (LHC) and from a soybean mutant containing reduced amounts of LHC were compared to wild type chloroplasts of the same species to determine the involvement of LHC in: 1) cation regulation of excitation energy distribution ("spillover") as determined by chlorophyll fluorescence in isolated chloroplasts, 2) light-induced slow fluorescence quenching in isolated plastids, 3) preillumination-induced state 1-state 2 adaptation of chloroplasts *in vivo*, and 4) the characteristics of the fluorescence transients of chloroplasts *in vivo*. The increase of photosystem II fluorescence induced by cations, slow fluorescence quenching and state 1-state 2 adaptation were not detected in the barley mutant and were reduced in the soybean mutant as compared to the wild type. These data suggest that the LHC is required for the regulation of spill-over of excitation energy between the photosystems. The characteristic I-D dip and P-S decay of the *in vivo* fluorescence induction curve (Kautsky effect) was not altered in the mutant chloroplasts as compared to that of the corresponding wild type plastids, indicating that these characteristics of the transient are not (necessarily) associated with the spill-over.

F-AM-F12 SINGLET EXCITON DIFFUSION PROPERTIES IN CHLOROPLASTS. C.E. Swenberg, N.E. Geacintov, Dept. of Chemistry, New York University, N.Y., N.Y. and J. Breton*, Sevice de Biophysique, Department of Biology, Saclay, France.

Prompt fluorescence emission at 735 nm and 680 nm from spinach chloroplasts was measured as a function of the intensity of the incident single picosecond laser pulse for several temperatures from 21°K to 300°K. The fluorescence was excited by a dye laser operated with the dye Rhodamine 6G with mode locking achieved with the dye DODCI. A Pockels cell was used to select a single pulse. The observed fluorescence quenching with increasing pulse intensity, at a given temperature, was found to be the same from the two photosynthetic units. This quenching of fluorescence is interpreted theoretically in terms of singlet-singlet exciton annihilation. For the temperature range studied the quenching curves obeyed the equation, $\log (1+I)/I$, where I is an appropriate normalized intensity of excitation. A detail analysis of the data provides evidence that the singlet exciton has a diffusion length of about 700 A°.

F-AM-F13 AB INITIO QUANTUM MECHANICAL STUDIES ON THE EXCITED SINGLET AND TRIPLET STATES OF PHOTOSYNTHETIC SYSTEMS. J. D. Petke,* G. M. Maggiora, and R. E. Christoffersen,* Departments of Biochemistry and Chemistry, University of Kansas, Lawrence, Kansas 66045.

Ab Initio self-consistent field molecular orbital configuration interaction calculations (including multiply-excited configurations) have been carried out on the low lying singlet and triplet excited states of magnesium porphine, magnesium chlorin, and their corresponding free bases as a prelude to similar calculations on ethyl chlorophyllide a and ethyl pheophorbide a. A comparison of calculated spectral parameters such as singlet-singlet and triplet-triplet transition energies and oscillator strengths, Q and B band splittings, and singlet-triplet splittings will be made with available experimental data, along with an analysis of the configurational parentage and electronic structure of the various states. A discussion of the state diagrams of these molecules will also be presented.